

# Earth's Future

## RESEARCH ARTICLE

10.1029/2023EF004124

### Key Points:

- We developed a combined modeling approach to quantify the effects of compound drought and extreme temperature (DET) on wheat yield
- Annual average DET intensity contributed an additional 6% of Australia's wheat yield variation beyond univariate drought, heat, and frost intensities
- In extreme low-yield years, annual average DET intensity dominated wheat yield loss, with relative contribution exceeding 50%

### Supporting Information:

Supporting Information may be found in the online version of this article.

### Correspondence to:

B. Wang, D. L. Liu, and Q. Yu,  
[bin.a.wang@dpi.nsw.gov.au](mailto:bin.a.wang@dpi.nsw.gov.au);  
[de.li.liu@dpi.nsw.gov.au](mailto:de.li.liu@dpi.nsw.gov.au);  
[yuq@igsnr.ac.cn](mailto:yuq@igsnr.ac.cn)

### Citation:

Li, S., Wang, B., Liu, D. L., Chen, C., Feng, P., Huete, A., & Yu, Q. (2026). Compound drought and temperature events intensify wheat yield loss in Australia. *Earth's Future*, 14, e2023EF004124. <https://doi.org/10.1029/2023EF004124>

Received 26 SEP 2023  
 Accepted 31 OCT 2025

### Author Contributions:

**Conceptualization:** Siyi Li, Bin Wang  
**Formal analysis:** Siyi Li  
**Methodology:** Siyi Li, Bin Wang, De Li Liu, Chao Chen, Qiang Yu  
**Software:** Siyi Li, De Li Liu, Puyu Feng  
**Supervision:** Bin Wang, De Li Liu, Alfredo Huete, Qiang Yu  
**Visualization:** Siyi Li  
**Writing – original draft:** Siyi Li  
**Writing – review & editing:** Bin Wang, De Li Liu, Chao Chen, Puyu Feng, Alfredo Huete

© 2026. The Author(s).

This is an open access article under the terms of the [Creative Commons Attribution License](#), which permits use, distribution and reproduction in any medium, provided the original work is properly cited.

## Compound Drought and Temperature Events Intensify Wheat Yield Loss in Australia

Siyi Li<sup>1,2,3</sup> , Bin Wang<sup>3,4</sup>, De Li Liu<sup>3,4,5</sup> , Chao Chen<sup>6</sup>, Puyu Feng<sup>7</sup> , Alfredo Huete<sup>2</sup> , and Qiang Yu<sup>1</sup> 

<sup>1</sup>College of Agriculture, Shanxi Agricultural University, Taigu, Shanxi, China, <sup>2</sup>School of Life Sciences, Faculty of Science, University of Technology Sydney, Sydney, NSW, Australia, <sup>3</sup>NSW Department of Primary Industries, Wagga Wagga Agricultural Institute, Wagga Wagga, NSW, Australia, <sup>4</sup>Gulbali Institute (Agriculture, Water and Environment), Charles Sturt University, Wagga Wagga, NSW, Australia, <sup>5</sup>Climate Change Research Centre, University of New South Wales, Sydney, NSW, Australia, <sup>6</sup>CSIRO Agriculture and Food, Wembley, WA, Australia, <sup>7</sup>College of Land Science and Technology, China Agricultural University, Beijing, China

**Abstract** The escalation in extreme weather events has raised concerns for agriculture. The quantification of the impacts of extreme events on crop yield has predominantly concentrated on individual events like drought or heat. Numerous instances have showcased the destructive effects of compound extreme events on crop yields, surpassing those of individual events. However, their influence extent is region-specific and not fully understood in Australia's crop belt. Using a biophysical-statistical modeling approach, we quantified the individual impacts of drought, heat, frost, and compound drought and extreme temperature (DET) events on wheat yield variations in Australia. We first developed indices for these different extreme events during the wheat reproductive period based on the APSIM (Agricultural Production System sIMulator) model and then used these indices in multiple linear regression models to quantify their impacts on wheat yield variations. We found that, during 1990–2021, drought, heat, and frost events explained 48% of yield variation, while the percentage increased to 54% after including DET events, with some regions even up to 86%. In extreme low-yield years, the relative importance of DET events surpassed the sum importance of individual drought, heat, and frost events, reaching 52% in years with yields below the 10th percentiles, respectively. Our findings highlight the need to factor compound extreme weather events into climate risk management to inform the mitigation of yield losses or crop failure.

**Plain Language Summary** Global warming has brought more extreme weather events like drought, heatwaves, frost, etc. These extreme events seriously threaten agricultural production and food security, especially multiple co-occurring weather events, which usually cause far more destructive effects than individual ones. In this study, we used a combined modeling approach to precisely quantify the impacts of individual and co-occurring extreme weather events on wheat yield variation over the past three decades in Australia. We found that these extreme weather events were responsible for more than half of the wheat yield variation, with multiple co-occurring extreme weather events particularly responsible for severe wheat yield losses in Australia. These findings highlight the need to factor co-occurring extreme weather events into climate risk management to inform the mitigation of yield losses or crop failure.

## 1. Introduction

Extreme weather events are key drivers of grain production variability (Iizumi & Ramankutty, 2016). For instance, they contributed 18%–43% of the inter-annual yield variation for the top four crops in the world (maize, wheat, rice, and soybeans) during 1961–2008 (Vogel et al., 2019). Over the past decades, there has been a notable rise in the frequency and intensity of extreme events (Manning et al., 2019; Myhre et al., 2019; Zwiers et al., 2013), with more co-occurrence of multiple extremes in both space and time (Hao et al., 2022; Lesk & Anderson, 2021; Sarhadi et al., 2018). Such increases in compound extreme events are projected to continue or even escalate under future climate change (Wang et al., 2023). The compound extreme events can present severe challenges to agricultural cropping systems. They give rise to more extreme situations than individual extreme events (drought, heat, or frost) (AghaKouchak et al., 2020) and generally cause more damaging impacts (Cohen et al., 2021; E. Li et al., 2022; S. Li et al., 2022). For example, during the summer of 2018 in Europe, compound drought-heat events resulted in widespread crop harvest failure across many European countries (Bastos

et al., 2020). In 2016, France experienced the most severe crop yield loss in the past half-century due to the combination of abnormally wet and hot climate conditions (Ben-Ari et al., 2018). Additionally, the simultaneous occurrence of frost and drought led to a wheat harvest failure in about 12% of the cropping area across Brazil in the late spring of 2006 (Júnior et al., 2021).

Compound drought and extreme temperature (DET) events are defined as the simultaneous occurrence of multiple climate-related hazards, including drought, heat, and frost. DET events are categorized as multivariate events according to the typology of compound weather and climate events proposed by Zscheischler et al. (2020). Compared to other compound events, the simultaneous co-occurrence of drought and extreme temperature events has more serious adverse impacts on crops (E. Li et al., 2022; S. Li et al., 2022; Potopová et al., 2021) and there is much more specific case evidence to link them with especially poor crop harvests (Christian et al., 2020; Ciais et al., 2005; Júnior et al., 2021; Lesk et al., 2022; Yuan et al., 2018). Thus, it is critically important to understand the characteristics of DET events and their impacts on crops, which is of great significance for assisting crops to adapt to climate change and realizing a stable increase in crop yields.

Australia is one of the top wheat exporters, consistently contributing about 11% of global wheat exports since 1961 (FAO, 2020). Nevertheless, Australian wheat generally relies on seasonal rainfall, making it highly susceptible to climate variability (Feng, Wang, Liu, et al., 2022; Feng, Wang, Macadam, et al., 2022). During the past decades, recurring drought in Australia has resulted in large wheat yield losses (Chenu et al., 2013; Feng et al., 2020). The untimely radiation frost in spring (Marcellos & Single, 1975) and the increasing heat events around wheat flowering and grain-filling stages (Ababaei & Chenu, 2020) both can simultaneously co-occur with drought, therefore aggravating the adverse impacts on wheat. However, the previous studies on the impacts of extreme events on Australian wheat were based on single extreme events (Ababaei & Chenu, 2020; Feng et al., 2018; Madadgar et al., 2017; Telfer et al., 2018). To our knowledge, no study has quantified the impacts of DET events on wheat yield in Australia's crop belt. Therefore, a robust assessment of the impacts of DET events on wheat yield is urgently needed for a more comprehensive understanding of climate risks facing grain production in Australia.

Different methods have been used to assess the impacts of DET events on crop yields over the past two decades (Lesk et al., 2022; E. Li et al., 2022; S. Li et al., 2022; Potopová et al., 2021). One approach is to compare the yield for specific years when compound extreme events occur with normal-year yield, proving that compound extreme events are the major drivers of severe yield losses (Beillouin et al., 2020; Ben-Ari et al., 2018). For example, comparing the yields of wheat and maize in Europe between 2003 and 2002 (normal year) demonstrated that compound drought and heat in 2003 led to yield drops of 11%–21% (García-Herrera et al., 2010). This method offers a clear and direct comparison of crop yields before and after compound drought and heat events. However, it is limited to specific instances or short timeframes, failing to capture the long-term magnitude and implications of compound extreme events impacts. By contrast, the assessment method based on the joint distributions using copula and cloud models can demonstrate the long-term impacts of compound extremes on crop yields (Feng & Hao, 2020; P. Feng et al., 2019; S. Feng et al., 2019). Ribeiro et al. (2020) constructed a trivariate joint distribution of maximum temperature, precipitation, and wheat/barley yields with nested copulas. They found that from 1989 to 2016 in Spain, compound dry and hot conditions resulted in an additional yield loss likelihood of 8%–29% compared to individual drought or heat events. However, these studies only obtain the probabilities or likelihood of the yield loss led by compound extremes. The third approach combined joint distribution with response function to quantify the long-term impacts of compound events on crops (Potopová et al., 2021; Simanjuntak et al., 2023; Zampieri et al., 2017). For example, according to the yield response function estimated with time and joint distribution of heat and drought from 1981 to 2015 in the United States, the impact of heat stress on maize yields has been amplified up to fourfold when coupled with water stress (Haqqi et al., 2021). This approach, which lacks quantification of compound events, resembles an analysis that merely adds the responses to two individual extreme events. However, the impacts of compound events are not the sum of the impacts of their individual components (Cohen et al., 2021). Additionally, present studies primarily focused on the impacts of compound extreme events on summer maize, with limited studies addressing the long-term implications for winter wheat. (Hamed et al., 2021; Haqqi et al., 2021; Lesk et al., 2021; Luan et al., 2021).

Process-based biophysical models are pivotal tools in agricultural science, providing insights into the complex interactions between the environment, management practices, and crop genotypes (Chenu et al., 2017). They have been widely applied in analyzing the impacts of both historical and future climate extreme events on crops across various regions around the world (Cammarano & Tian, 2018; Harrison et al., 2016; Mangani et al., 2019; van der

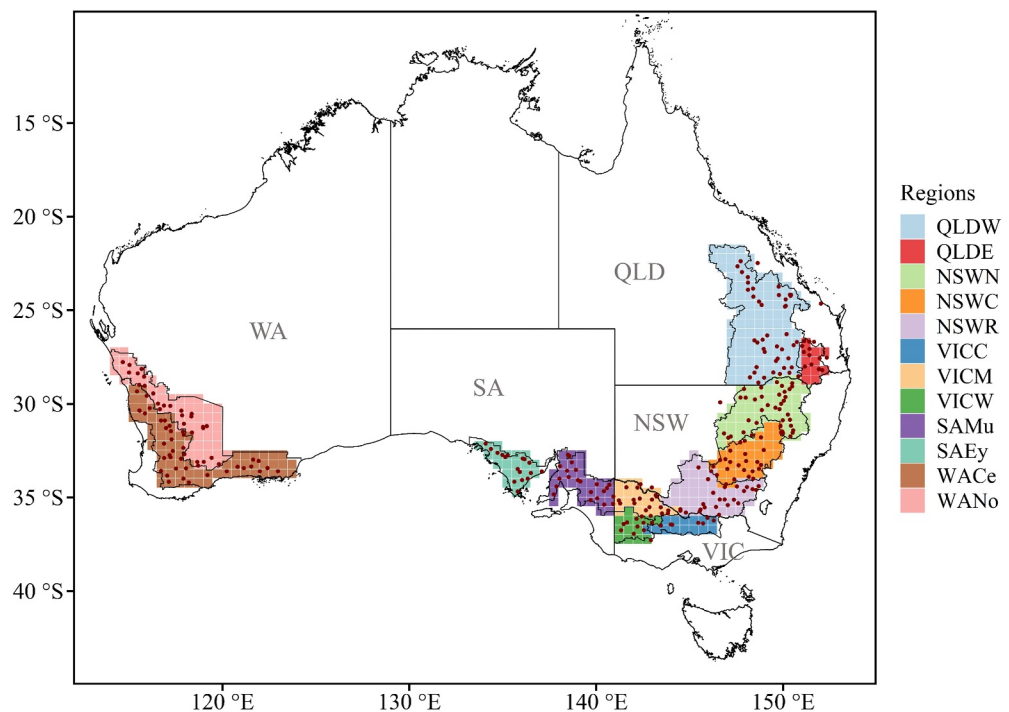


**Figure 1.** The map of Australia's crop belt includes 12 subregions (refer to Table 1 for full name of region acronyms) and 453 grids ( $0.5^\circ \times 0.5^\circ$ ). The red dots represent 296 soil locations used for the APSIM (Agricultural Production System iMulator) model. WA: Western Australia, SA: South Australia, QLD: Queensland, NSW: New South Wales, VIC: Victoria.

Velde et al., 2012). Although biophysical models can integrate the various mechanisms that influence crop growth during extreme events, the oversimplification of certain processes may lead to inaccurate results (Eitzinger et al., 2013; Watson et al., 2017). Combining biophysical models with statistical analysis leverages the strengths of both, blending mechanistic and empirical statistical models (Keating & Thorburn, 2018). Roberts et al. (2017), P. Feng et al. (2019), and S. Feng et al. (2019) have shown that integrating biophysical and statistical models performs better than either model alone.

Here, we quantified the long-term impacts of both individual and compound drought and extreme temperature events on wheat yield in Australia's crop belt from 1990 to 2021, using a biophysical-statistical modeling approach. Biophysical-statistical modeling approach allows capturing extreme weather events (drought, heat, frost, and DET events) that occur during the wheat reproductive period (WRP), providing a basis for quantifying their long-term impacts. We aim to (a) study the characteristics of individual and DET events during 1990–2021; (b) quantify the impacts of individual and DET events on wheat yield variation in 12 subregions in the Australian crop belt; (c) identify the relative importance of individual and DET events to wheat yield variation during low-yield years. We expect the findings from this study will aid the climate impacts assessment, to offer more comprehensive insights and clear directions for better risk assessment and management within the agricultural industry.

## 2. Materials and Methods

### 2.1. Study Area

Our study area was the Australian crop belt, which is across the eastern, southeastern, and western parts of Australia (Xie et al., 2024). It contains 12 Australian Bureau of Agricultural and Resource Economics and Sciences (ABARES) classification regions (Figure 1 and Table 1). Since the crop belt spans a wide range of latitude and longitude, it has a large precipitation and temperature gradient. The annual cumulative rainfall (1990–2021) increased from 302.6 mm in the inland area to 641.1 mm closer to the coastal region, and the average temperature rose from 14.8°C in the south to 21.2°C in the north. Wheat, the most important crop in Australia's crop belt, normally is grown under rainfed conditions during April–November (Wang, Li Liu, et al., 2018; Wang, Liu, et al., 2018).

**Table 1**  
Mean Wheat Yield, Annual Cumulative Rainfall, and Mean Temperature in 12 Subregions of Australia's Crop Belt During 1990–2021

| Subregions                                     | Yield (t/ha) | Rainfall (mm)   | Tmean (°C)   |
|------------------------------------------------|--------------|-----------------|--------------|
| QLD Western Downs and Central Highlands (QLDW) | 1.41 (0.49)  | 550.16 (191.40) | 21.17 (0.60) |
| QLD Eastern Darling Downs (QLDE)               | 2.00 (0.79)  | 641.06 (173.40) | 18.32 (0.51) |
| NSW North West Slopes and Plains (NSWN)        | 1.83 (0.81)  | 547.53 (169.29) | 18.88 (0.61) |
| NSW Central West (NSWC)                        | 1.83 (0.83)  | 563.26 (172.98) | 16.89 (0.58) |
| NSW Riverina (NSWR)                            | 2.37 (0.92)  | 445.79 (139.96) | 16.67 (0.55) |
| VIC Central North (VICC)                       | 2.35 (0.93)  | 510.57 (147.29) | 15.05 (0.52) |
| VIC Mallee (VICM)                              | 1.63 (0.64)  | 302.60 (98.57)  | 16.81 (0.46) |
| VIC Wimmera (VICW)                             | 2.42 (0.91)  | 452.48 (105.11) | 14.81 (0.47) |
| SA Murray Lands and Yorke Peninsula (SAMu)     | 2.14 (0.58)  | 352.88 (91.92)  | 16.35 (0.40) |
| SA Eyre Peninsula (SAEy)                       | 1.46 (0.46)  | 341.21 (83.33)  | 17.33 (0.40) |
| WA Central and Southern Wheat Belt (WACe)      | 1.91 (0.34)  | 422.34 (90.52)  | 17.26 (0.41) |
| WA Northern and Eastern Wheat Belt (WANO)      | 1.37 (0.36)  | 311.36 (82.73)  | 19.00 (0.52) |

*Note.* Values in the bracket are the standard deviation.

## 2.2. Data Sources

We downloaded the historical (1990–2021) gridded climate data from Scientific Information for Land Owners (SILO, 2023). It provides gridded daily rainfall, maximum temperature, minimum temperature, and radiation at a resolution of 0.05° throughout Australia. From this data set, we extracted 41,534 grid cells that fall within our study area. To balance computational efficiency with result accuracy, we upscaled these grid cells from 0.05 to 0.5° using the “raster” package of R. Grid upscaling involves aggregating the original fine-resolution raster cells into fewer, larger cells (Misaghian et al., 2018). Specifically, we started from the upper-left end of a raster, aggregating 10 raster cells in the horizontal direction and 10 cells in the vertical direction in to one larger cells by averaging the values in all 10 × 10 cells (Feng, Wang, Liu, et al., 2022; Feng, Wang, Macadam, et al., 2022).

Soil hydraulic properties and soil parameters were derived from the APSoil database (Apsoil, 2022). APSoil is primarily developed to offer location-specific soil input data for use in the APSIM (Agricultural Production System sIMulator) model. It provides a complete set of soil data required for running APSIM (Dagliaiesh et al., 2012). 296 soil sites were selected to ensure that each climate-data grid has a corresponding soil profile that is geographically closest to its center point.

Actual wheat yield data in 12 ABARES regions were obtained from the commodities survey statistics from 1990 to 2021 (ABARES, 2023). ABARES, the research arm of the Australian Government Department of Agriculture, Fisheries and Forestry, provides professionally independent data, research, analysis, and advice to inform public and private decisions affecting Australian agriculture, fisheries, and forestry. In this study, we employed yield anomaly (Equation 1) to quantify the contribution of weather extremes on yield variation, aiming to represent the magnitude of deviation from the mean yield in annual absolute yields in each region (Schauberger et al., 2017).

$$\Delta Y_{xt} = Y_{xt} - \bar{Y} \quad (1)$$

where  $Y_{xt}$  is the wheat yield in region  $x$  for  $t_{th}$  year and  $\bar{Y}$  is the mean wheat yield across all regions over the period 1990–2021.

## 2.3. APSIM Simulation

APSIM version 7.10 (Holzworth et al., 2014) was used in this study. APSIM is a modeling framework that describes the biophysical process of the agricultural system (Keating et al., 2003). It has been applied and well-validated in numerous studies of the Australian wheat production system (Asseng et al., 2011; Feng, Wang, Liu,

et al., 2022; Feng, Wang, Macadam, et al., 2022). We used climate data and soil information to drive APSIM at 0.5° grid cell from 1990 to 2021. State-specific sowing windows and corresponding wheat cultivars were established (Table S1 in Supporting Information S1) following previous studies in the same study area (Feng, Wang, Liu, et al., 2022; Feng, Wang, Macadam, et al., 2022; Wang, Li Liu, et al., 2018; Wang, Liu, et al., 2018). Wheat sowing occurred within the window when either the accumulated rainfall exceeded 25 mm over 7 consecutive days or the sowing window was coming to an end. The fertilizer applied at sowing was 130 kg ha<sup>-1</sup> of urea, which is equivalent to 60 kg ha<sup>-1</sup> of Nitrogen. The data output from APSIM simulations, including date, wheat phenology, and daily plant available water (PAW: measured in millimeters), served as intermediary variables for calculating the intensity of drought, heat, frost, and compound drought and extreme temperature events during the WRP.

## 2.4. Drought, Heat, Frost, and Compound Drought and Extreme Temperature

First, we defined the three types of individual extreme events: drought, heat, and frost. We defined drought as a condition in which the water content in the 0–100 cm soil layer is lower than 40% of plant available water capacity (PAWC) for three or more consecutive days. PAWC represents the total amount of water a soil can store for crops to use. It is calculated as the difference in volumetric water content between the upper drainage limit (DUL) and crop (wheat) lower limit (wheat LL) (Asseng et al., 2001; Wang et al., 2017). Previous studies have shown that when the amount of extractable soil water for wheat is below 40% of PAWC, the stomatal conductance, root growth, tiller number, and yield of wheat can decrease (Ciais et al., 2005; Granier et al., 1999; Kirkegaard & Lilley, 2007). We defined drought using PAW, diverging from traditional methods employed for the calculation of well-established drought indices such as the Standardized Precipitation Index (SPI) (Stagge et al., 2015). Our definition of drought was made based on two considerations. One is the definition of compound events in our study is anchored in the individual extreme event definitions, necessitating the exclusion of drought indices based on monthly or seasonal scales to realize the development of daily scale compound event indices. The other one is that PAW is directly correlated with crop uptake, directly influencing crop development and growth. It integrates the effects of soil characteristics, precipitation, and evapotranspiration, thereby providing a direct measure of the soil moisture deficit.

Heat was defined as a condition where the daily maximum temperature is higher than a threshold of 28°C for three or more consecutive days, causing both the size and weight of wheat grain to decrease (Lalic et al., 2013; Wheeler et al., 1996). As for frost, we used 2°C as the threshold to define frost events (Liu et al., 2011). This is consistent with Farre et al. (2010), who reported that when a daily minimum temperature was below 2°C during wheat flowering, it would cause yield loss.

Typically, during the wheat growth period in Australia, heat and frost do not co-occur; however, droughts frequently co-occur with either heat or frost. DET events were defined as the simultaneous occurrence of drought and heat, or drought and frost, in both time and space. According to the typology of compound events developed by Zscheischler et al. (2020), DET events fall under the category of 'multivariate events'. This category refers to the co-occurrence of multiple climate drivers and/or hazards in the same location causing an impact.

Based on the above definitions, we identified the occurrence of each drought, heat, frost, and DET event during the WRP from the initial floral stage to the end of the grain filling stage. The reason why we choose the WRP instead of the whole wheat growth season is that these extreme events are far more harmful when they occur in the WRP than in other growth stages (Cohen et al., 2021). To separate the effects of individual extremes from those of compound extreme events, individual drought, heat, or frost events were picked when DET did not occur (Table 2).

### 2.4.1. Daily Intensity of Drought, Heat, Frost, and DET

We aimed to create normalized 0–1 intensity metrics for drought, heat, frost, and DET events at the daily scale during the WRP for each grid cell across Australia's crop belt. The daily drought intensity for each grid cell is represented by the difference between the drought threshold ( $\delta \times PAWC_n$ ) and the daily PAW divided by the drought threshold. It is a dimensionless value between 0 and 1, DI is 1 when PAW<sub>ni</sub> = 0, representing the highest drought intensity (Equation 2).

**Table 2**

Example of One Compound Drought and Extreme Temperature (DET) Event Occurred in the Wheat Reproductive Period (WRP)

| Day of year ( $d_i$ ) | PAW (mm) | Tmax (°C) | Tmin (°C) | DET |
|-----------------------|----------|-----------|-----------|-----|
| 215 ( $w_s$ )         | 49.8     | 21.2      | 0.4       | NO  |
| ...                   | 45.9     | 22.6      | 0.6       | NO  |
| ...                   | 42.6     | 24.2      | -2.4      | NO  |
| 275 ( $l+1$ )         | 40.5     | 23.0      | -3.1      | YES |
| 276 (...)             | 39.5     | 21.3      | -1.9      | YES |
| 277 ( $l+m$ )         | 36.4     | 25.3      | -0.5      | YES |
| 278                   | 33.7     | 23.6      | 2.6       | NO  |
| 279                   | 31.3     | 24.6      | 4.0       | NO  |
| 280                   | 29.2     | 27.2      | 3.3       | NO  |
| 281 ( $l+1$ )         | 27.2     | 29.9      | 5.5       | YES |
| 282 (...)             | 25.4     | 30.8      | 8.6       | YES |
| 283 ( $l+m$ )         | 24.8     | 30.5      | 8.4       | YES |
| ...                   | 42.9     | 31.1      | 4.9       | NO  |
| ...                   | 43.8     | 33.4      | 2.9       | NO  |
| 300 ( $w_e$ )         | 46.5     | 30.7      | 7.6       | NO  |

Note.  $d_i$  is the  $i$ th day in the WRP;  $w_s$  and  $w_e$  are the start day and the end day of the WRP, respectively,  $l$  is the day before the start of the DET event,  $m$  represents the number of days each DET event lasts. The thresholds for drought, heat, and frost events in this example are 41.9 mm, 28°C, and 2°C, respectively.

$$DI_{ni} = \begin{cases} 0, & PAW_{ni} \geq \delta \times PAWC_n \\ \frac{\delta \times PAWC_n - PAW_{ni}}{\delta \times PAWC_n}, & PAW_{ni} < \delta \times PAWC_n \end{cases}^i \\ = l+1, l+2, \dots, l+m, m \geq 3 \quad (2)$$

where  $DI_{ni}$  is the daily drought intensity in the grid  $n$  for the  $i$ th day during WRP in a given year, the subscript  $l$  denotes the day before the start of each extreme event ( $i = l+1, l+2, \dots, l+m$ ,  $m \geq 3$  is for representing the requirement of 3 or more consecutive days for each type of extreme events);  $\delta \times PAWC_n$  is the threshold to define drought according to extractable water, in which  $PAWC_n$  is decided by soil properties in the grid  $n$ ,  $\delta$  is 0.4 in this study;  $PAW_{ni}$  is the plant available water in grid  $n$  on the  $i$ th day during the WRP.

The daily heat intensity for each grid cell was calculated using Equation 3. The ratio of  $Tmax$  exceeding of the heat threshold ( $T_c$ ) to the wheat high killing temperature ( $T_s$ ) exceeding of  $T_c$  was calculated as the heat intensity. Also, it is a dimensionless value between 0 and 1, with 1 representing the highest heat intensity when  $Tmax_{ni} = T_s$ .

$$HI_{ni} = \begin{cases} 0, & Tmax_{ni} \leq T_c \\ \frac{Tmax_{ni} - T_c}{T_s - T_c}, & T_c < Tmax_{ni} < T_s \quad i = l+1, l+2, \dots, l+m, m \geq 3 \\ 1, & Tmax_{ni} \geq T_s \end{cases} \quad (3)$$

where  $HI_{ni}$  is the daily heat intensity in the grid  $n$  for the  $i$ th day during WRP in a given year;  $Tmax_{ni}$  is the maximum temperature in the grid  $n$  for the  $i$ th day during the WRP;  $T_c$  is the heat threshold temperature, which was taken as 28°C. We took  $T_s$  (the wheat high killing temperature) as 42°C, based on Kumar Tewari and Charan Tripathy (1998) who pointed out that wheat was killed when exposed to 42°C for more than 48 hr.

The daily frost intensity for each grid cell was calculated using Equation 4. The ratio of the difference between  $Tmin$  and the frost threshold ( $T_t$ ) to the difference between wheat low killing temperature ( $T_r$ ) and  $T_t$  was calculated as the frost intensity. Also, it is a dimensionless value between 0 and 1, with 1 representing the highest frost intensity when  $Tmin_{ni} = T_r$ .

$$FI_{ni} = \begin{cases} 0, & Tmin_{ni} \geq T_t \\ \frac{Tmin_{ni} - T_t}{T_r - T_t}, & T_r < Tmin_{ni} < T_t \quad i = l+2, \dots, l+m, m \geq 3 \\ 1, & Tmin_{ni} \leq T_r \end{cases} \quad (4)$$

where  $FI_{ni}$  is the daily frost intensity in the grid  $n$  for the  $i$ th day during WRP in a given year;  $Tmin_{ni}$  is the minimum temperature in the grid  $n$  for the  $i$ th day during the WRP;  $T_t$  is the frost threshold temperature, which we took as 2°C. We took  $T_r$  (the wheat low killing temperature) as -5°C (Single, 1985).

The definition of DET can be expressed below:

$$DET_{ni} = (DI_{ni} \geq 0) \& (HI_{ni} \geq 0) \& (FI_{ni} \geq 0), i = l+1, l+2, \dots, l+m, m \geq 3 \quad (5)$$

where  $DET_{ni}$  is the  $i$ th day within a DET event for the grid  $n$ .

The daily DET intensity was obtained by weighing the sum of the daily standardized values of intensity of compound drought-heat events and the intensity of compound drought-frost events (Equation 6). Frost and heat

events do not occur simultaneously in the WRP in our calculation. Frost typically occurs in the early WRP, while heat events occur in the middle to late WRP. This pattern is due to the WRP in Australia spanning from spring to summer. As a result, we set the weights for DI and HI to add up to 1, and the weights for DI and FI to also add up to 1.

$$\text{DETI}_{ni} = \alpha \times \text{DI}_{ni} + \begin{cases} (1 - \alpha) \times \text{HI}_{ni}, & i = l + 1, l + 2, \dots, l + m, m \geq 3 \\ (1 - \alpha) \times \text{FI}_{ni} & \end{cases} \quad (6)$$

where  $\text{DETI}_{ni}$  is the daily intensity of DET in the grid  $n$  for the  $i_{th}$  day of a given year;  $\alpha$  is the weight for daily drought intensity, we used 0.5, it can be adjusted according to sufficient Supporting Information S1.

#### 2.4.2. Annual Intensity of DET, Drought, Heat, and Frost

The annual DET intensity for each grid cell ( $\text{DETI}_n$ ) was obtained by adding the cumulative sum of the daily intensity of all DET days in the WRP in each grid cell. Drought, heat, and frost were obtained by excluding the DET episodes. The annual drought intensity ( $\text{DI}_n$ ), heat intensity ( $\text{HI}_n$ ), and frost intensity ( $\text{FI}_n$ ) in each grid cell were the cumulative sum of daily drought intensity ( $\text{DI}_{ni}$ ), heat intensity ( $\text{HI}_{ni}$ ), and frost intensity ( $\text{FI}_{ni}$ ), respectively, on all non-DET days in the WRP. After calculating the annual  $\text{DI}_n$ ,  $\text{HI}_n$ ,  $\text{FI}_n$ , and  $\text{DETI}_n$  in 453 grid cells across Australia's crop belt, we computed the spatial average of these indices for all grids within each subregion to represent the intensity of each extreme event type (DI, HI, FI, and DETI) for that specific subregion. Then the region-level DI, HI, FI, and DETI were combined with wheat yield anomaly to establish the relationship.

#### 2.5. Trends in Annual Intensity Over Time

We applied the Mann-Kendall trend test on DI, HI, FI, and DETI to evaluate the statistical significance of their time series trends in each subregion. The standardized test statistic  $Z$  was employed to indicate the trend status, where a positive  $Z$  value signifies an increasing trend in the time series, while a negative  $Z$  value shows a decreasing trend. Time series trends are considered statistically significant at the 5% significance level (corresponding to 95% confidence interval) if  $|Z| > 1.96$  Han et al., 2018; E. Li et al., 2022; S. Li et al., 2022).

#### 2.6. Impacts of Annual DET Intensity on Wheat Yield Variation

We employed four sets of multiple linear regression (MLR) models to comprehensively assess the influence of DETI on wheat yield variations across Australia. The first set was to identify the contribution of DETI in wheat yield anomalies at national scale. One model included only individual extreme indices as independent variables (Equation 8), whereas the other incorporated both individual and compound extreme indices (Equation 7). These models were fitted using data on annual wheat yield anomalies and extreme indices over 32 years in 12 regions (384 data points).

$$\Delta Y_{xt} = \beta_0^{xt} + \beta_1^{xt} \text{DI}_{xt} + \beta_2^{xt} \text{HI}_{xt} + \beta_3^{xt} \text{FI}_{xt} + \beta_4^{xt} \text{DETI}_{xt} + \delta_x + \varepsilon_{xt} \quad (7)$$

$$\Delta Y_{xt} = \beta_0^{xt'} + \beta_1^{xt'} \text{DI}_{xt} + \beta_2^{xt'} \text{HI}_{xt} + \beta_3^{xt'} \text{FI}_{xt} + \delta_x' + \varepsilon_{xt}' \quad (8)$$

where  $\Delta Y_{xt}$  denotes yield anomaly in the region  $x$  for  $t_{th}$  year;  $\text{DI}_{xt}$ ,  $\text{HI}_{xt}$ ,  $\text{FI}_{xt}$ , and  $\text{DETI}_{xt}$  are the standardized DI, HI, FI, and DETI in the region  $x$  for  $t_{th}$  year;  $\delta_x$  and  $\delta_x'$  are region fixed effects in models with and without DETI, respectively;  $\varepsilon_{xt}$  and  $\varepsilon_{xt}'$  are error terms.

A second set of MLR models was developed to evaluate the contribution of DETI in positive and negative wheat yield anomaly at national scale. we divided the data set (32 years  $\times$  12 regions = 384 data points) into positive (189 data points) and negative (195 data points) yield anomaly years, and then fitted MLR models both with and without DETI (Equations 9–12).

$$\Delta Y_{xp} = \beta_0^{xp} + \beta_1^{xp} \text{DI}_{xp} + \beta_2^{xp} \text{HI}_{xp} + \beta_3^{xp} \text{FI}_{xp} + \beta_4^{xp} \text{DETI}_{xp} + \delta_{xp} + \varepsilon_{xp} \quad (9)$$

$$\Delta Y_{xp} = \beta_0^{xp'} + \beta_1^{xp'} \text{DI}_{xp} + \beta_2^{xp'} \text{HI}_{xp} + \beta_3^{xp'} \text{FI}_{xp} + \delta_{xp}' + \varepsilon_{xp}' \quad (10)$$

where  $\Delta Y_{xp}$  is yield anomaly in the region  $x$  for  $p_{th}$  year of positive yield anomaly years;  $DI_{xp}$ ,  $HI_{xp}$ ,  $FI_{xp}$ , and  $DETI_{xp}$  are the standardized DI, HI, FI, and DETI in the region  $x$  for  $p_{th}$  year of positive yield anomaly years;  $\delta_{xp}$  and  $\delta_{xp}'$  are region fixed effects in models with and without DETI, respectively;  $\epsilon_{xp}$  and  $\epsilon_{xp}'$  are error terms.

$$\Delta Y_{xn} = \beta_0^{xn} + \beta_1^{xn} DI_{xn} + \beta_2^{xn} HI_{xn} + \beta_3^{xn} FI_{xn} + \beta_4^{xn} DETI_{xn} + \delta_{xn} + \epsilon_{xn} \quad (11)$$

$$\Delta Y_{xn} = \beta_0^{xn'} + \beta_1^{xn'} DI_{xn} + \beta_2^{xn'} HI_{xn} + \beta_3^{xn'} FI_{xn} + \delta_{xn}' + \epsilon_{xn}' \quad (12)$$

where  $\Delta Y_{xn}$  is yield anomaly in the region  $x$  for  $n_{th}$  year of negative yield anomaly years;  $DI_{xn}$ ,  $HI_{xn}$ ,  $FI_{xn}$ , and  $DETI_{xn}$  are the standardized DI, HI, FI, and DETI in the region  $x$  for  $n_{th}$  year of negative yield anomaly years;  $\delta_{xn}$  and  $\delta_{xn}'$  are region fixed effects in models with and without DETI, respectively;  $\epsilon_{xn}$  and  $\epsilon_{xn}'$  are error terms.

The third set of MLR models were performed separately in each region to characterize the impacts of DETI at regional scale. Similarly, models with and without DETI were both run in each region (2 models  $\times$  12 regions = 24 regressions with 32 points in each region):

$$\Delta Y_t = \beta_0^t + \beta_1^t DI_t + \beta_2^t HI_t + \beta_3^t FI_t + \beta_4^t DETI_t + \epsilon_t \quad (13)$$

$$\Delta Y_t = \beta_0^t' + \beta_1^t' DI_t + \beta_2^t' HI_t + \beta_3^t' FI_t + \epsilon_t' \quad (14)$$

where  $\Delta Y_t$  is yield anomaly for  $t_{th}$  year in each region;  $DI_t$ ,  $HI_t$ ,  $FI_t$ , and  $DETI_t$  are the standardized DI, HI, FI, and DETI for  $t_{th}$  year in each region;  $\delta_t$  and  $\delta_t'$  are region fixed effects in models with and without DETI, respectively;  $\epsilon_t$  and  $\epsilon_t'$  are error terms.

The fourth set of MLR models focused on five levels of low-yield years, identified by the 10th, 20th, 30th, 40th, and 50th percentiles of yield anomalies across all 384 data points. The wheat yield anomaly at each level and corresponding DI, HI, FI, and DETI were fitted in the MLR model to quantify the relative importance of each variable for each low-yield level.

$$\Delta Y_p = \beta_0^p + \beta_1^p DI_p + \beta_2^p HI_p + \beta_3^p FI_p + \beta_4^p DETI_p + \epsilon_p \quad (15)$$

where  $\Delta Y_p$  is yield anomaly for  $p_{th}$  year in each level of low-yield years;  $DI_p$ ,  $HI_p$ ,  $FI_p$ , and  $DETI_p$  are the standardized DI, HI, FI, and DETI for  $p_{th}$  year in low-yield years;  $\delta_p$  and  $\delta_p'$  are region fixed effects in models with and without DETI, respectively;  $\epsilon_p$  and  $\epsilon_p'$  are error terms.

For all MLR models, the adjusted determination coefficient ( $R^2$ ) is a statistical metric used to measure the goodness of fit for regression models, improving upon the traditional determination coefficients. It incorporates an adjustment factor based on the number of predictors in the model and the total number of predictors, helping to identify which variables are truly beneficial to the model. Adjusted  $R^2$  is particularly useful for comparing the simulation results of models that have different predictors.

We utilized the metric “lmg” from the R package “relaimpo” (Groemping, 2006) to calculate the relative importance of each independent variable. The “lmg” method provides a decomposition of the model-explained variance into non-negative contributions (Groemping & Matthias, 2018). It considers all possible orders in which the independent variables can enter the regression model. For each order, it calculates the increase in  $R^2$  when a variable is added to the model. These contributions are then averaged across all possible orders to derive the final “lmg” score for each predictor, which represents its relative importance. To mitigate the impact of differing magnitudes of predictors on the “lmg” results, we standardized all predictors to have a mean of zero and a variance of one before performing the regression.

## 2.7. Assumption Tests for Multiple Linear Regression Models

Before model fitting, we calculated the variance inflation factor (VIF) to detect potential multicollinearity among the independent variables in each of the 12 subregions. The VIF measures how much the variance of the estimated regression coefficient is inflated due to multicollinearity, with values ranging from 1 to  $+\infty$ . A VIF of 1 indicates that there is no multicollinearity among variables, and the larger the VIF, the stronger the multicollinearity among

**Table 3**

*The Relative Frequencies (%) of Drought (D), Heat (H), Frost (F), Compound Drought and Extreme Temperature (DET), Compound Drought and Heat (D + H), and Compound Drought and Frost (D + F) Days During the Wheat Reproductive Period (the Average Duration Was 81 Days) for 12 Subregions*

| Subregions                                     | D  | H | F | DET | D + H | D + F |
|------------------------------------------------|----|---|---|-----|-------|-------|
| QLD Western Downs and Central Highlands (QLDW) | 53 | 1 | 2 | 26  | 22    | 4     |
| QLD Eastern Darling Downs (QLDE)               | 58 | 0 | 4 | 15  | 11    | 4     |
| NSW North West Slopes and Plains (NSWN)        | 53 | 1 | 3 | 18  | 17    | 1     |
| NSW Central West (NSWC)                        | 47 | 0 | 3 | 11  | 10    | 1     |
| NSW Riverina (NSWR)                            | 52 | 1 | 2 | 10  | 10    | 0     |
| VIC Central North (VICC)                       | 44 | 1 | 2 | 5   | 5     | 0     |
| VIC Mallee (VICM)                              | 39 | 1 | 2 | 4   | 4     | 0     |
| VIC Wimmera (VICW)                             | 67 | 0 | 1 | 8   | 8     | 0     |
| SA Murray Lands and Yorke Peninsula (SAMu)     | 57 | 0 | 1 | 6   | 6     | 0     |
| SA Eyre Peninsula (SAEy)                       | 60 | 1 | 0 | 5   | 5     | 0     |
| WA Central and Southern Wheat Belt (WACe)      | 51 | 1 | 0 | 6   | 6     | 0     |
| WA Northern and Eastern Wheat Belt (WANo)      | 69 | 1 | 0 | 15  | 15    | 0     |
| Mean value                                     | 54 | 1 | 2 | 11  | 10    | 1     |

variables (Liu et al., 2019). The VIFs of the independent variables in MLR models were from 1.01 to 2.79 across 12 subregions (Table S2 in Supporting Information S1), suggesting that there was no significant multicollinearity among the variables.

Assumption tests in linear regression analysis are crucial for ensuring reliability and validity, including independence of errors, normality, and homoscedasticity. We performed the Durbin-Waston test, Shapiro-Wilk test, and Breusch-Pagan test to check the independence of errors, normality, and homoscedasticity, respectively, in the MLR for all regions combined and for each region (Donati & Amais, 2019; Khasawneh & Al-Oqaily, 2023; Steinskog et al., 2007). The significance level for these assumptions was 0.05. If the p-value was less than 0.05, the corresponding assumption was rejected. The test results indicated that the null hypothesis of normality and homoscedasticity were satisfied in MLR models for each of the 12 regions separately, as well as for all regions combined. However, in the MLR models for the NSWR and SAMu regions, the null hypothesis of error independence was rejected.

To evaluate the statistical significance of the improvement in explaining yield anomalies after including DETI in MLR, we performed a likelihood ratio test based on the analysis of variance and the Akaike Information Criterion (AIC) (Lewis et al., 2011; Murtaugh, 2014).

### 3. Results

#### 3.1. The Frequency of Drought, Heat, Frost, and DET During the WRP

Table 3 illustrates the relative frequencies of various extreme events during the WRP, including the frequencies of drought (D), heat (H), frost (F), compound drought and extreme temperature events (DET), compound drought and heat (D + H), and compound drought and frost (D + F). The average duration of the WRP was 81 days. The results showed that drought events exhibited the highest frequency across all regions, with an average frequency of 54%. In contrast, heat and frost events were much less frequent, averaging 1% and 2%, respectively. DET occurred with an average frequency of 11%, though there were notable regional variations, ranging from 4% to 26%. Among the DET components, D + H was significantly more frequent than D + F in all regions, indicating that D + H was a more prevalent component of DET compared to D + F.

#### 3.2. Spatial and Temporal Characteristics of Drought, Heat, Frost, and DET

Figure 2 shows the temporal variations of annual DI, HI, and FI during the WRP from 1990 to 2021. The most pronounced fluctuations of DI were observed in three regions within Victoria, with DI values ranging

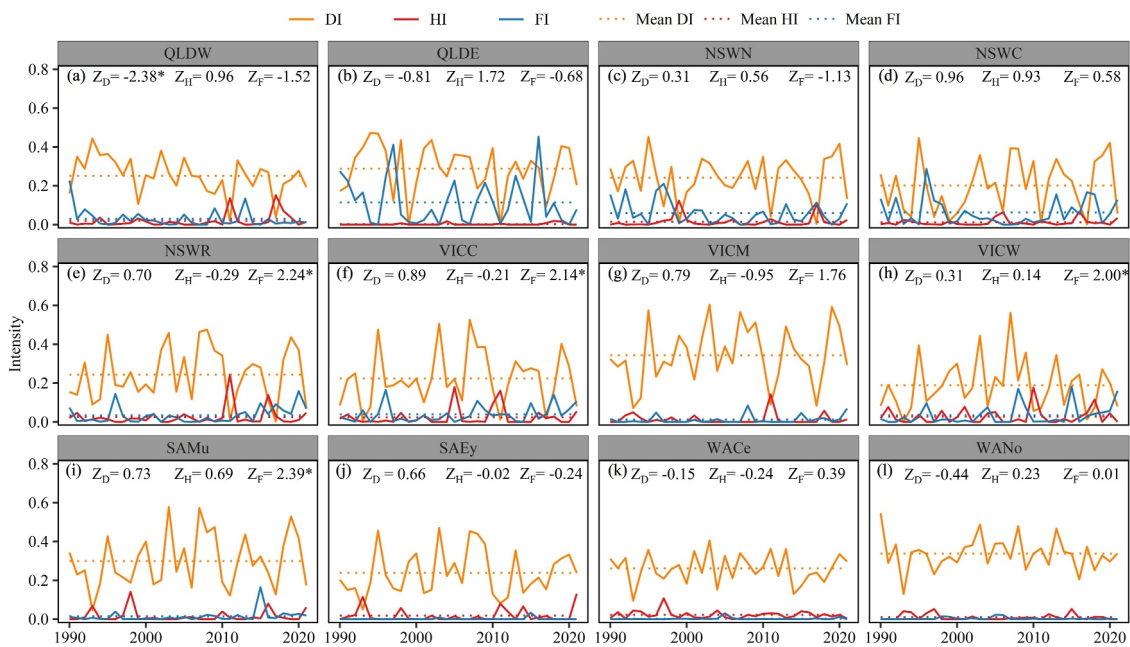


**Figure 2.** Temporal variations of drought intensity, heat intensity, and frost intensity during the WRP from 1990 to 2021 in 12 regions across Australian crop belt.  $Z_D$ ,  $Z_H$ , and  $Z_F$  are the increasing (decreasing) rates of drought intensity (DI), heat intensity (HI), and frost intensity (FI) from 1990 to 2021, respectively (\*\* $p < 0.001$ , \*\* $p < 0.01$ , \* $p < 0.05$ ).

from 0.01 to 0.53 in VICC, 0.07 to 0.60 in VICM, and 0 to 0.56 in VICW (Figures 2f–2h). In contrast, the variations in *DI* were the smallest in Western Australia, ranging from 0.10 to 0.41 in WACe and 0.13 to 0.55 in WANo (Figures 2k and 2l). The long-term (1990–2021) annual mean of *DI* was highest in VICM and WANo, with a value of 0.34 (Figures 2g and 2l). Conversely, the lowest annual mean *DI* was recorded at 0.19 in VICW (Figure 2h). From 1990 to 2021, the *HI* generally remained low across all regions, typically close to 0. The greatest year-to-year variation in *HI* occurred in NSWR (Figure 2e), ranging from 0 to 0.24. It was followed by VICC and VICW (Figures 2f and 2h), each with a range from 0 to 0.18. On average, VICW and NSWR recorded the highest annual mean *HI* at 0.03 (Figures 2h and 2e), while QLDW had the lowest mean *HI* at 0.002 (Figure 2b). Temporal variations in *FI* showed noticeable fluctuations in most regions, with QLDW exhibiting the most significant variations, ranging from 0 to 0.45 (Figure 2b). While in regions of SAMu, SAEy, WACe, and WANo, the *FIs* were consistently low to nearly 0 (Figures 2i–2l). The multi-year average *FI* was highest at 0.11 in QLDW (Figure 2b) and was lowest at around 0.002 in three western subregions (SAEy, WACe, and WANo) (Figures 2j–2l).

The temporal variations of DETI are displayed in Figure 3 alongside the wheat yield variations. DETI also exhibited fluctuations throughout the period from 1990 to 2021 in all 12 regions. The most pronounced fluctuations of DETI were exhibited in QLDW, with values ranging from 0.01 to 0.61 (Figure 3a), while the region of SAEy showed the slightest fluctuations, with values ranging from 0 to 0.15 (Figure 3j). Based on the multi-year average DETI, the region QLDW experienced the highest DETI, with a value of 0.33 (Figure 3a), while the region VICW and SAEy had the lowest DETI, both at 0.06 (Figures 3g and 3j). Additionally, wheat yield anomalies varied greatly from year to year. Except for the two regions of QLDW and SAMu (Figures 3a and 3i), the wheat yield anomaly showed significantly negative correlations with DETI. The highest correlation coefficients were in the three regions that belong to New South Wales (NSW), with values of -0.66 and -0.72, respectively (Figures 3c–3e).

The spatial distribution of mean *DI*, *HI*, *FI*, and DETI during 1990–2021 in the Australian crop belt is presented in Figure 4. The values of *DI* ranged from 0 to 0.62, which were slightly higher in inland areas. The western part of NSW and Western Australia (WA) had the highest mean *DI* (Figure 4a). The *HI* within the WRP ranged widely from 0.0006 to 0.28, a few grid cells located east and south of the crop belt experienced high *HI* values, while most of the crop belt had low *HI* values (Figure 4b). There was also a wide range in *FI*, 0.0003–0.22, which gradually

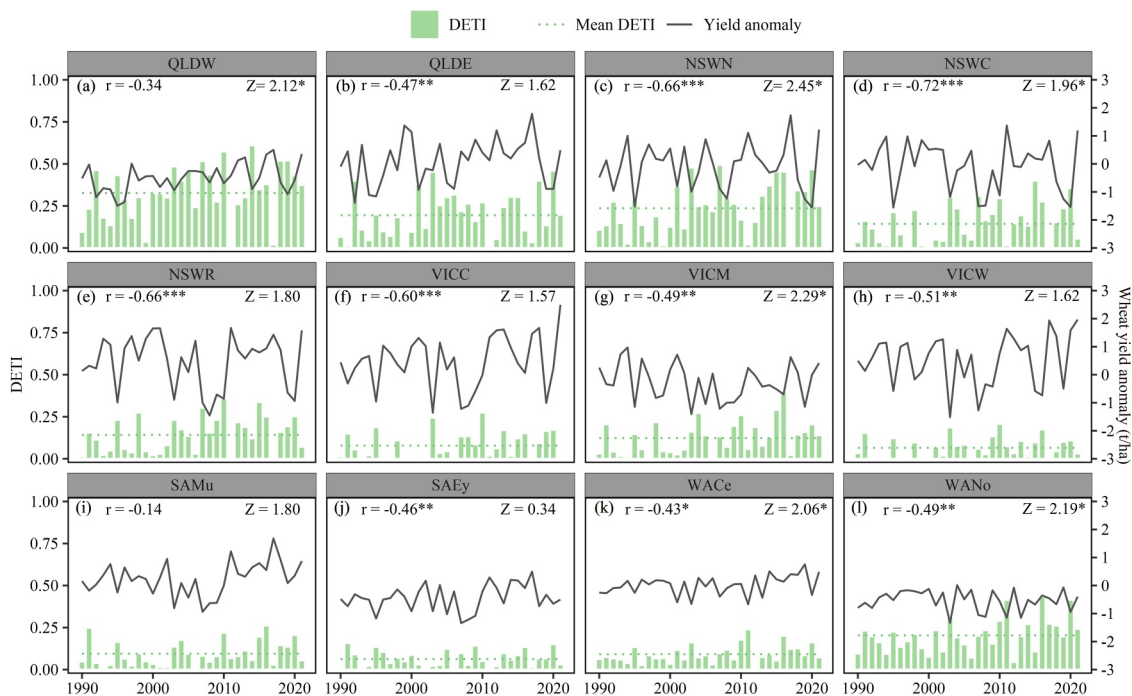


**Figure 3.** Wheat yield anomaly and intensity of compound drought and extreme temperature events (DETI) over the 12 regions in Australia from 1990 to 2021.  $r$  is the correlation coefficient between wheat yield anomaly and DETI.  $Z$  is the increasing (decreasing) rates of DETI from 1990 to 2021 (\*\* $p$  < 0.001, \*\* $p$  < 0.01, \* $p$  < 0.05).

increased from west to east of the Australian crop belt (Figure 4c). The DETI values ranged from 0 to 0.50 across Australia's crop belt, representing a north-south gradient that gradually decreased (Figure 4d).

### 3.3. The Impacts of Extreme Weather Events on Wheat Yield Variation During 1990–2021

Figures 5a and 5b shows the comparison between actual and estimated wheat yield anomalies for all regions combined. The individual drought, heat, and frost could explain 48% of wheat yield variation across Australia (Figure 5a). After including the index of DETI, the accuracy in reproducing the actual wheat yield anomaly of the MLR model was increased to 54% (Figure 5b), which means that DETI can account for 6% wheat yield variation across Australia. Particularly, the estimated wheat yield anomaly in Australia's crop belt was closer to the actual yield anomaly during the years with negative yield anomalies (Figures 5a–5d). In essence, the improvement of adjusted  $R^2$  resulting from DETI mainly comes from low-yield years (Figures 5a–5d).

The adjusted  $R^2$  values for MLR models with and without DETI as an independent variable for 12 subregions and all regions combined are shown in Figure 5e. The impacts of individual and compound drought and extreme temperature events varied across different regions. Without DETI, three single extreme indices could explain 12%–85% yield variation of 12 subregions with the highest adjusted  $R^2$  in region NSW and the smallest one in region QLDW. When including DETI as an additional variable in the MLR model, the values of adjusted  $R^2$  increased for most regions, ranging from 0.17 to 0.86. This implies that the inclusion of DETI improved the ability of the model to explain the anomaly in wheat yield caused by extreme weather events in Australia's crop belt. Notably, there were significant model improvements in QLDW, NSW, VICM, VICW, WANo, and all regions combined after including DETI as a predictor (Figure 5e), and this improvement was the greatest in the WANo region.

To compare the contribution of different extreme indices to wheat yield variation, we obtained the relative importance of DI, HI, FI, and DETI in each region from the MLR model (Figure 5f). The values of relative importance varied across different regions, with the range of 0.33–0.82 in DI, 0.01–0.15 in HI, 0.003–0.10 in FI, and 0.03–0.44 in DETI. Except for the region of QLDW, DI was consistently regarded as the most important

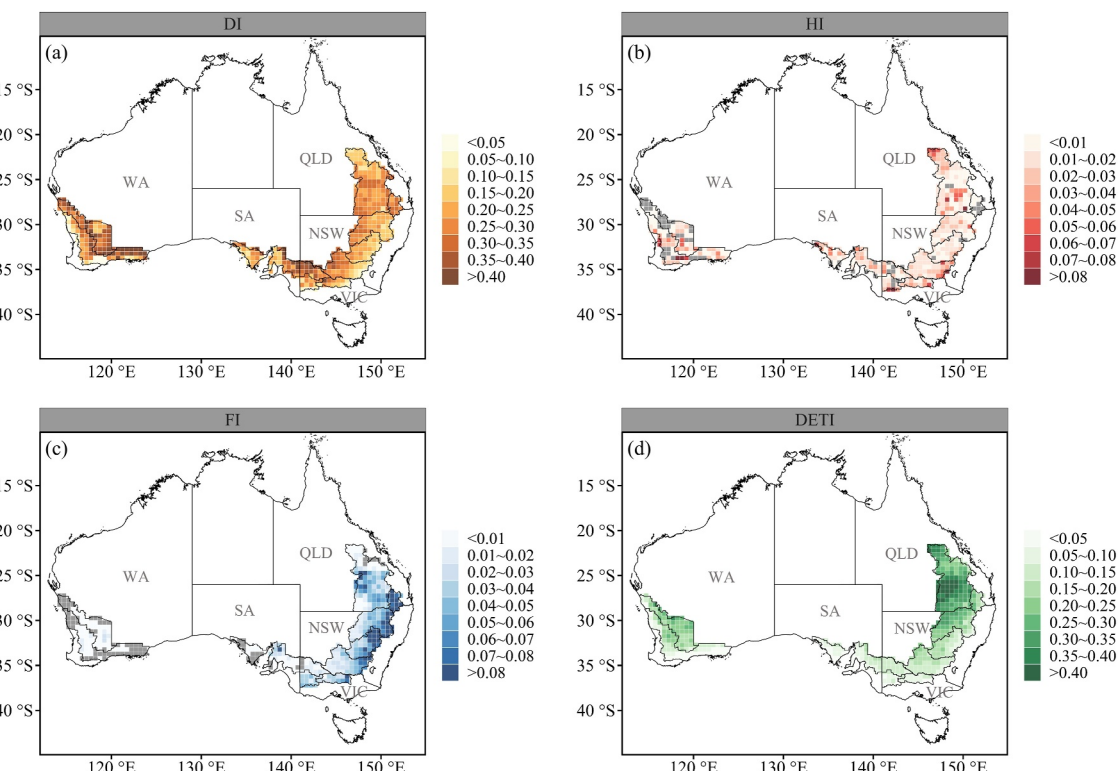


**Figure 4.** Spatial distributions of average intensity of drought (DI), heat (HI), frost (FI), and compound drought and extreme temperature events (DETI) during the wheat reproductive growth period in 1990–2021 across Australia's crop belt. The gray grids indicate where there are no extreme weather events.

index for all regions. The DETI was the second most important index. The relative importance of HI and FI were similar and demonstrated the lowest values in all regions, except for the SAMu region.

#### 3.4. The Contribution of Extreme Weather Events in Low-Yield Years

The relative importance of DI, HI, FI, and DETI for each low-yield level is shown in Figure 6. We found that DETI dominated the wheat yield variation in extremely low-yield years (10th percentile), the relative importance exceeded 50%, surpassing the combined contribution of DI, HI, and FI. However, in the other levels of low-yield years, DI became the dominant factor influencing yield variation, with importance ranging from 70% to 74%, while DETI showed less importance than DI at 18%–23%. Additionally, the relative importance of HI and FI were 5%–14% and 1%–5%, respectively, which were much lower than that of DI or DETI in all levels of low-yield years. But both HI and FI exhibited their highest relative importance in extremely low-yield years (10th) compared to moderate low-yield years.

## 4. Discussion

We analyzed the intensity of drought, heat, frost, and DET events, and assessed the impacts of DETI on wheat yields in Australia from 1990 to 2021. The DI had great inter-annual variations across entire Australia's crop belt in the past 30 years, and DI exhibited higher values in subregions located near inland areas. The spatial-temporal distribution of DI was consistent with previous studies (Chenu et al., 2013; Feng et al., 2020; Hu et al., 2020). In terms of the HI and FI, as the season shifts from spring to summer during the stage of wheat floral initial to the end of grain-filling, frost events gradually decrease while heat events increase (Zheng et al., 2012). In addition, in the mid-late period of the WRP (flowering and grain filling), drought events are more frequent. Therefore, there was a higher frequency of heat events coinciding with drought events compared to frost events (Table S7 and Figure S2 in Supporting Information S1) (Chenu et al., 2013). This is the reason why, after removing the period of DET, the

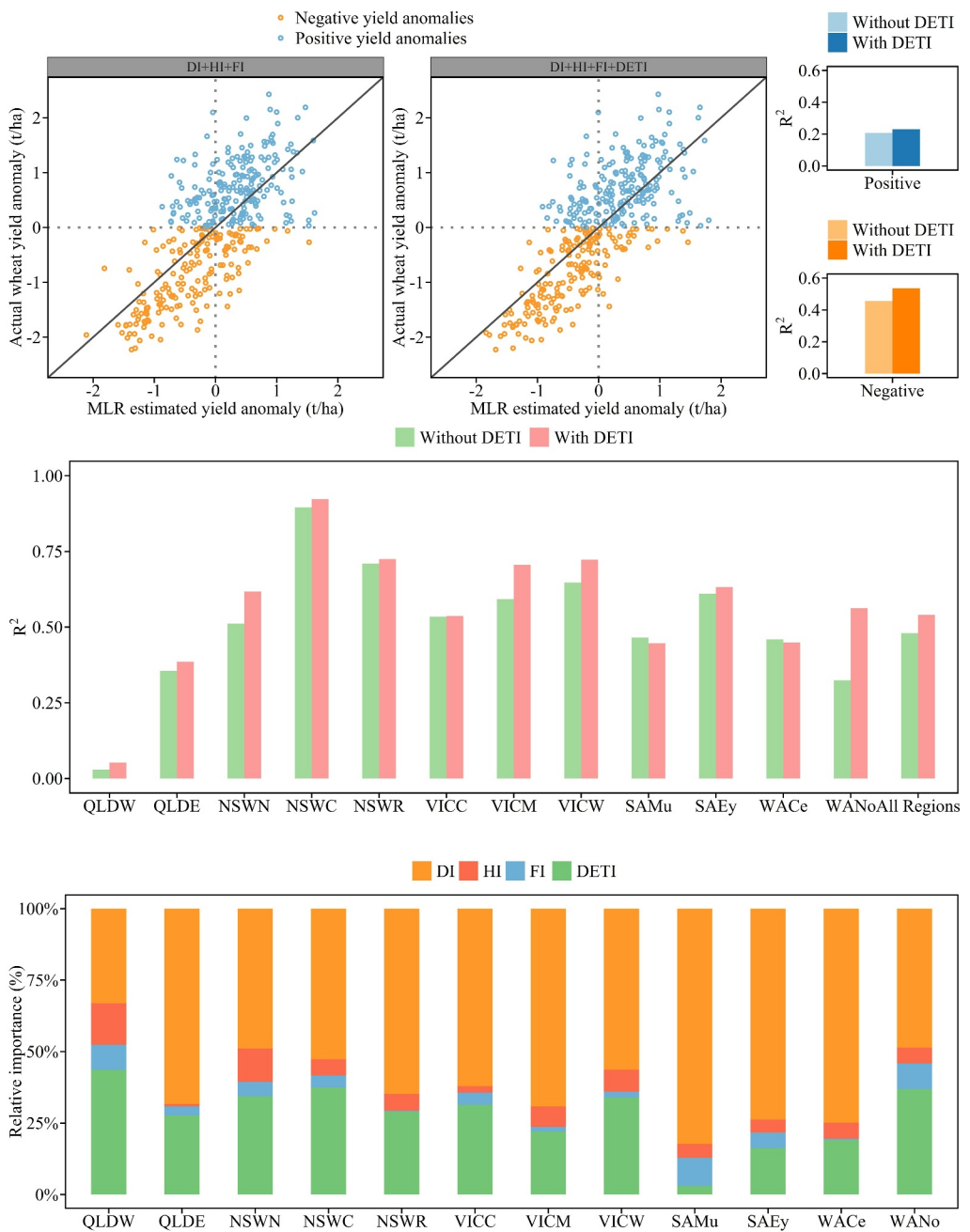


**Figure 5.** The comparison between observed wheat yield anomalies and values estimated with multiple linear regression (MLR) models using two sets of extreme weather events from 1990 to 2021 in Australia's crop belt: (a) observed versus estimated yield variation based on the indices of drought intensity (DI) + heat intensity (HI) + frost intensity (FI), (b) observed versus estimated yields based on the indices of DI + HI + FI + DETI intensity (DETI), (c) the adjusted determination coefficients ( $R^2$ ) of MLR in estimating wheat yield variation with and without DETI for positive yield anomalies of all regions combined, and (d) for negative yield anomalies of all regions combined, (e) in 12 subregions, and (f) the relative importance of extreme climate indices to wheat yield variation in 12 subregions based on multiple linear regression models. Numbers on each pair of bars represent the difference in adjusted  $R^2$  between MLR models with and without DETI, and \* denotes a  $p$ -value lower than 0.05 in the variance analysis.

HI was low across the entire crop belt (Figure 4b), while the FI was similar to the frost intensity containing the period of DET (Chenu et al., 2013; Zheng et al., 2012), which was higher in the eastern part and lower in the western part of the crop belt (Figure 4c).

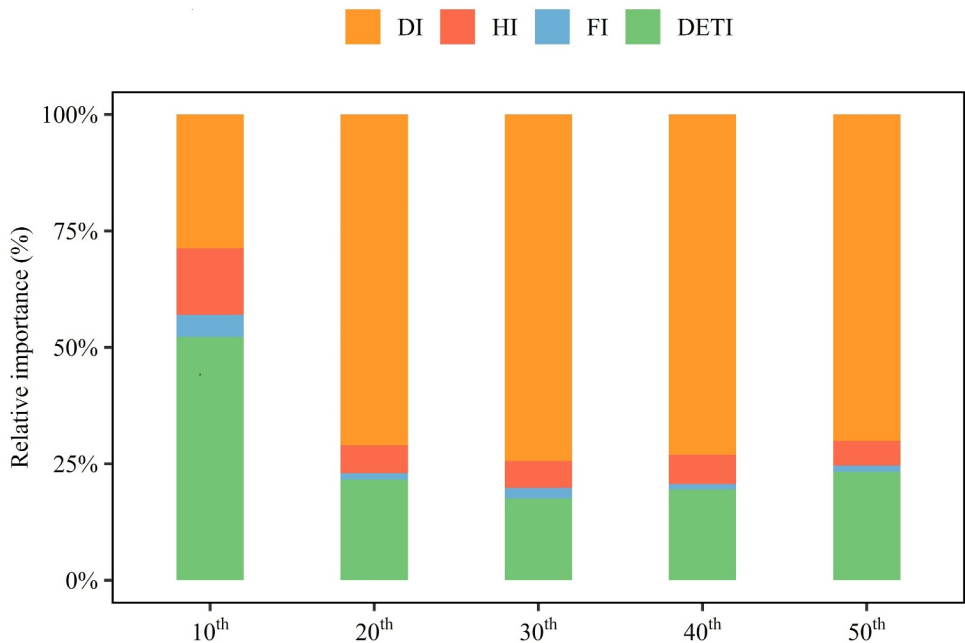


**Figure 6.** Relative importance of extreme weather events to wheat yield variation in low-yield years determined by different percentiles of wheat yields in Australia's crop belt. FI: frost intensity, HI: heat intensity, DI: drought intensity, DETI: intensity of compound drought and extreme temperature events.

Between 1990 and 2021, there was an increased DETI in all 12 subregions (Figure 3). Notably, regions of QLDW, NSWN, NSWC, VICM, WACe, and WANo exhibited particularly pronounced increases during this period. This upward trend could be attributed to a combination of increasing drought and heat occurrences (Figure S2 in Supporting Information S1). Spatially, the DETI exhibited a decreasing gradient from north to south of Australia's crop belt, aligning with the distribution of the maximum temperature during the WRP (Figure S1a in Supporting Information S1), which was consistent with the distribution of heat events in the previous study in the same study area (Collins & Chenu, 2021). Therefore, it is evident that the spatial distribution of DETI in Australia's crop belt was dominated by the extreme high temperature.

Regarding the 12 subregions, the explanations of individual and compound drought and extreme temperature events were region-specific (Figure 5e). The adjusted  $R^2$  was both low before and after including DET events in QLDW and QLDW, indicating that the impacts of extreme weather events on wheat yield variation in Queensland were not as great as in other states. This divergence could be attributed to the fact that, unlike the winter-dominant rainfall in other states, Queensland has a summer-dominant rainfall pattern (Backhouse & Burgess, 2002; Wang et al., 2020). Moreover, the clay soils with large water-holding capacity in that region are capable of storing sufficient rainfall before the wheat sowing season, therefore buffering the adverse impacts of climate (Nix & Fitzpatrick, 1969; Wang, Li Liu, et al., 2018). In the other 10 subregions, the most notable increments in adjusted  $R^2$  were observed in NSWN, VICM, and WANo, with values of 0.11, 0.11, and 0.24 respectively. This phenomenon could be attributed to these regions having the highest DETI values within their respective states. Particularly noteworthy, WANo exhibited the most substantial increase in adjusted  $R^2$  upon the inclusion of DETI. This is likely because Western Australia is predominantly characterized by sandy soil, which is prone to structural degradation (Hamza & Anderson, 2002) and has a lower water capacity compared to other states in Australia (Padarian et al., 2014). Consequently, the soil buffer in Western Australia is limited, making it more susceptible to DET compared to other regions.

The relative importance of drought, heat, frost, and DET to wheat yield variation during 1990–2021 was similar across the 12 subregions (Figure 5f). Except for QLDW, drought contributed the most in the other 11 subregions, all exceeding 50%. It is not surprising that drought is the primary impact event for the long-term wheat yield variation in Australia, as Australia's crop belt is located in arid and semi-arid areas, and wheat mainly relies on seasonal rainfall (Wang et al., 2020). Lobell et al. (2015) predicted that the yield losses attributed to drought

would consistently be higher than that of other extreme events in the coming half-century. Note that DET was the second most important event impacting the wheat yield variation in Australia. Generally, compound extreme events can have more severe impacts on crops than individual extreme events (Cohen et al., 2021; Ribeiro et al., 2020), while the relative importance of DET was lower than that of drought in our study. This difference might be attributed to the fact that compound extreme events have a higher level of extremity compared to individual extreme events, their duration and frequency could be lower than individual extreme events in the same growth period. Meanwhile, in a continuous long-time series, high-intensity compound events did not occur every year. As shown in Figure 3, there were more years with below-average DETI than years with above-average DETI.

Considering the greater impact of DETI on years with negative yield anomalies (Figures 5a–5d), we selected different levels of low-yield years based on the percentiles of the data set encompassing all years across the 12 subregions to evaluate the corresponding relative importance of each extreme event to wheat yield anomaly. Notably, in the extreme low-yield years (years of wheat yield lower 10th), the relative importance of DETI was the highest, which not only exceeded that of DI but even surpassed the sum of the importance of DI, HI, and FI (Figure 6). This agrees well with the previous studies that linked severe yield loss with compound temperature and moisture stress (Christian, Jordan I et al., 2020; García-Herrera et al., 2010; Glotter & Elliott, 2016; Wegren, 2011). In this study, we calculated the mean DETI in low-yield years, which had yield anomalies lower than the 10th percentile, and the mean DETI value was 0.23. This value can be used as the threshold for assessing whether DET are likely to result in severe yield loss. By integrating this threshold with the robust prediction for extreme weather events, the early warning of severe yield loss is expected to be realized. This will serve as a reminder to policymakers and farmers to prioritize adapting to DET events, with the aim of mitigating or preventing significant yield losses or crop failures in Australia.

Planning appropriate agronomic adaptative strategies ahead of DET years might have great potential to alleviate the adverse impacts. For farmers, employing strategies such as selecting stress-tolerant cultivars, sowing at optimal times, implementing cover cropping, and practicing no-till farming contribute to enhancing crop resilience to DET events (Kaye & Quemada, 2017; Li et al., 2024; Semenov & Strattonovitch, 2015). Additionally, diversifying income sources, such as integrating livestock with crop production, exploring alternative farming activities, or cultivating a broader range of crop species, can further diminish risks (Hussain et al., 2020). For policymakers, it is imperative to enhance meteorological services and intensify efforts to effectively communicate these risks to farmers and other stakeholders (Anaman et al., 1995). Providing subsidies for heat- and drought-resistant crop seeds, water-efficient technologies, and agricultural equipment is crucial. Moreover, fostering a collaborative approach that engages local communities, agricultural experts, and government agencies is vital for developing comprehensive response strategies.

We assessed the impacts of DET events from 1990 to 2021 and identified the contribution of DET events to wheat yield variation in long-term series and low-yield years in Australia's crop belt. Nonetheless, there are some limitations that need to be considered. The analysis employed regional average wheat yield data, lacking information specific to local or individual farm levels. Additionally, due to the broad scope of wheat yield data, the wheat varieties and agricultural practices integrated into the APSIM model were also at a regional level. This approach might disregard variations in local cultivars and management techniques. However, this constraint underscores the significance of gathering and integrating more location-specific data to enhance the precision and applicability of future investigations. Second, this study is limited by its reliance on a single crop simulation model. Different crop models diverge in their foundational assumptions, algorithms, and parameter configurations. As a result, even when given identical inputs, they can produce disparate results (Asseng et al., 2013). It might be more robust to employ ensembles of multiple crop models to simulate crop growth and soil water dynamics, as this can yield more reliable outcomes (Rötter et al., 2015). This also emphasizes the need for localized data to facilitate the development of multiple models.

Third, different thresholds for drought, heat, and frost can influence the computed indices, leading to varying severities of these extreme events. Note that there are no certain thresholds set for inducing water, heat, and cold stress in wheat. For instance, He et al. (2022) set a high-temperature tolerance limit of 28°C during the wheat grain-filling stage, while Wardlaw et al. (2002) documented a significant reduction in kernel weight under heat stress conditions exceeding 32°C. Stone and Nicolas (1994) identified 35°C as the critical upper limit beyond which wheat tolerance notably decreases. Researchers should determine appropriate thresholds based on their

study's specific objectives and scope. Additionally, future studies could assess the diverse impacts of extreme events defined by different thresholds on crop yield, thereby providing insights for selecting thresholds in subsequent studies. Moreover, the weighting of DI and HI/FI in deriving DETI could be varied across Australia's crop belt and from the year 1990–2021. The assignment of weights is influenced by a range of factors, encompassing the intensity and timing of individual extremes, crop cultivars, soil characteristics, as well as the sensitivity and adaptability of diverse regions. Achieving reasonable weight allocation is a multifaceted challenge requiring significant multidimensional information support. In future studies, it may be prudent to treat weights as variables and undertake sensitivity analyses on a spatial scale.

## 5. Conclusion

Our study assessed the impacts of drought, heat, frost, and DET events on wheat yield variation in Australia's crop belt from 1990 to 2021, using the 12-subregion wheat yield data obtained from ABARES. We found that DETI had large inter-annual variation, with a slight increasing trend from 1990 to 2021. Spatially, it showed a decreasing gradient from north to south across Australia's crop belt. This spatial distribution was mainly dominated by high temperatures. Additionally, extreme weather events contributed 54% of wheat yield variation in the entire crop belt. Regarding the relative importance of DET events to wheat yield variation, it was second to that of drought in the long-term series. However, in extreme low-yield years, the relative importance of DET events surpassed the sum importance of individual drought, heat, and frost events, reaching 52% in years with yields below the 10th percentiles, respectively. Our findings highlight the significant impact of DET on the annual fluctuations in wheat yield, indicating its potential to cause significant yield losses in Australia. Our findings are expected to supplement the understanding of the impact of climate variability on the agricultural sector. Consequently, this information can be valuable for driving corresponding adaptive strategies, refining policy frameworks, and fostering technological innovations to strengthen agricultural resilience in the face of climate extremes.

## Conflict of Interest

The authors declare no conflicts of interest relevant to this study.

## Data Availability Statement

The climate and wheat yield data are publicly available from the following sources: the SILO climate data are at <https://www.longpaddock.qld.gov.au/silo/gridded-data/> and the wheat yield data are at <https://www.agriculture.gov.au/abares/data/farm-data-portal#data-download>. The code used in this work can be found at Li (2024b) and the processed data is available at Li (2024a).

## Acknowledgments

The first author acknowledges the China Scholarship Council (CSC) for the financial support for her Ph.D. study. Facilities for conducting this study were provided by the New South Wales Department of Primary Industries.

## References

Ababaei, B., & Chenu, K. (2020). Heat shocks increasingly impede grain filling but have little effect on grain setting across the Australian wheatbelt. *Agricultural and Forest Meteorology*, 284, 107889. <https://doi.org/10.1016/j.agrformet.2019.107889>

ABARES. (2023). Farm data portal—Beta—DAFF (agriculture.gov.au).

Aghakouchak, A., Chiang, F., Huning, L. S., Love, C. A., Mallakpour, I., Mazdiyasni, O., et al. (2020). Climate extremes and compound hazards in a warming world. *Annual Review of Earth and Planetary Sciences*, 48(1), 519–548. <https://doi.org/10.1146/annurev-earth-071719-055228>

Anaman, K. A., Thampapillai, D. J., Henderson-Sellers, A., Noar, P. F., & Sullivan, P. J. (1995). Methods for assessing the benefits of meteorological services in Australia. *Meteorological Applications*, 2(1), 17–29. <https://doi.org/10.1002/met.5060020104>

Apsoil. (2022). Retrieved from <https://www.longpaddock.qld.gov.au/silo/gridded-data/>

Asseng, S., Ewert, F., Rosenzweig, C., Jones, J. W., Hatfield, J. L., Ruane, A. C., et al. (2013). Uncertainty in simulating wheat yields under climate change. *Nature Climate Change*, 3(9), 827–832. <https://doi.org/10.1038/nclimate1916>

Asseng, S., Foster, J., & Turner, N. C. J. G. C. B. (2011). The impact of temperature variability on wheat yields. *Global Change Biology*, 17(2), 997–1012. <https://doi.org/10.1111/j.1365-2486.2010.02262.x>

Asseng, S., Turner, N., & Keating, B. a. J. P. (2001). Analysis of water-and nitrogen-use efficiency of wheat in a Mediterranean climate. *Plant and Soil*, 233(1), 127–143. <https://doi.org/10.1023/A:101038160223>

Backhouse, D., & Burgess, L. W. (2002). Climatic analysis of the distribution of Fusarium graminearum, F. pseudograminearum and F. culmorum on cereals in Australia. *Australasian Plant Pathology*, 31(4), 321–327. <https://doi.org/10.1071/AP02026>

Bastos, A., Ciais, P., Friedlingstein, P., Sitch, S., Pongratz, J., Fan, L., et al. (2020). Direct and seasonal legacy effects of the 2018 heat wave and drought on European ecosystem productivity. *Science Advances*, 6(24), eaba2724. <https://doi.org/10.1126/sciadv.aba2724>

Beillouin, D., Schauberger, B., Bastos, A., Ciais, P., & Makowski, D. (2020). Impact of extreme weather conditions on European crop production in 2018. *Philosophical Transactions of the Royal Society B*, 375(1810), 20190510. <https://doi.org/10.1098/rstb.2019.0510>

Ben-Ari, T., Boé, J., Ciais, P., Lecerf, R., Van Der Velde, M., & Makowski, D. (2018). Causes and implications of the unforeseen 2016 extreme yield loss in the breadbasket of France. *Nature Communications*, 9(1), 1627. <https://doi.org/10.1038/s41467-018-04087-x>

Cammarano, D., & Tian, D. (2018). The effects of projected climate and climate extremes on a winter and summer crop in the southeast USA. *Agricultural and Forest Meteorology*, 248, 109–118. <https://doi.org/10.1016/j.agrformet.2017.09.007>

Chenu, K., Dehifard, R., & Chapman, S. C. (2013). Large-scale characterization of drought pattern: A continent-wide modelling approach applied to the Australian wheatbelt—Spatial and temporal trends. *New Phytologist*, 198(3), 801–820. <https://doi.org/10.1111/nph.12192>

Chenu, K., Porter, J. R., Martre, P., Basso, B., Chapman, S. C., Ewert, F., et al. (2017). Contribution of crop models to adaptation in wheat. *Trends in Plant Science*, 22(6), 472–490. <https://doi.org/10.1016/j.tplants.2017.02.003>

Christian, J. I., Basara, J. B., Hunt, E. D., Otkin, J. A., & Xiao, X. (2020). Flash drought development and cascading impacts associated with the 2010 Russian heatwave. *Environmental Research Letters*, 15(9), 094078. <https://doi.org/10.1088/1748-9326/ab9faf>

Ciais, P., Reichstein, M., Viovy, N., Granier, A., Ogée, J., Allard, V., et al. (2005). Europe-wide reduction in primary productivity caused by the heat and drought in 2003. *Nature*, 437(7058), 529–533. <https://doi.org/10.1038/nature03972>

Cohen, I., Zandalinas, S. I., Huck, C., Fritschi, F. B., & Mittler, R. (2021). Meta-analysis of drought and heat stress combination impact on crop yield and yield components. *Physiologia Plantarum*, 171(1), 66–76. <https://doi.org/10.1111/ppl.13203>

Collins, B., & Chenu, K. (2021). Improving productivity of Australian wheat by adapting sowing date and genotype phenology to future climate. *Climate Risk Management*, 32, 100300. <https://doi.org/10.1016/j.crm.2021.100300>

Dalgliesh, N., Cocks, B., & Horan, H. (2012). APSoil-providing soils information to consultants, farmers and researchers. In *Paper presented at the 16th Australian Agronomy Conference, Armidale, NSW*.

Donati, G. L., & Amais, R. S. (2019). Fundamentals and new approaches to calibration in atomic spectrometry. *Journal of Analytical Atomic Spectrometry*, 34(12), 2353–2369. <https://doi.org/10.1039/C9JA00273A>

Eitzinger, J., Thaler, S., Schmid, E., Strauss, F., Ferrise, R., Moriondo, M., et al. (2013). Sensitivities of crop models to extreme weather conditions during flowering period demonstrated for maize and winter wheat in Austria. *The Journal of Agricultural Science*, 151(6), 813–835. <https://doi.org/10.1017/S0021859612000779>

FAO. (2020). The Food and Agriculture Organization of the United Nations. Retrieved from <https://www.fao.org/faostat/en/#data/QCL>

Farre, I., Foster, I., Biddulph, B., & Asseng, S. (2010). Is there a value in having a frost forecast for wheat in the South-West of Western Australia. In *Paper presented at the Food Security from Sustainable Agriculture: 15th Australian Agronomy Conference, Lincoln, New Zealand*.

Feng, P., Wang, B., Liu, D. L., Yu, Q., & Hu, K. (2022). Coupling machine learning with APSIM model improves the evaluation of climate extremes impact on wheat yield in Australia. In *Modeling Processes and Their Interactions in Cropping Systems: Challenges for the 21st Century* (pp. 251–275). <https://doi.org/10.1002/9780891183860.ch8>

Feng, P., Wang, B., Liu, D. L., Waters, C., & Yu, Q. (2019). Incorporating machine learning with biophysical model can improve the evaluation of climate extremes impacts on wheat yield in south-eastern Australia. *Agricultural and Forest Meteorology*, 275, 100–113. <https://doi.org/10.1016/j.agrformet.2019.05.018>

Feng, P., Wang, B., Liu, D. L., Xing, H., Ji, F., Macadam, I., et al. (2018). Impacts of rainfall extremes on wheat yield in semi-arid cropping systems in eastern Australia. *Climatic Change*, 147(3), 555–569. <https://doi.org/10.1007/s10584-018-2170-x>

Feng, P., Wang, B., Luo, J.-J., Liu, D. L., Waters, C., Ji, F., et al. (2020). Using large-scale climate drivers to forecast meteorological drought condition in growing season across the Australian wheatbelt. *Science of the Total Environment*, 724, 138162. <https://doi.org/10.1016/j.scitotenv.2020.138162>

Feng, P., Wang, B., Macadam, I., Taschetto, A. S., Abram, N. J., Luo, J.-J., et al. (2022). Increasing dominance of Indian Ocean variability impacts Australian wheat yields. *Nature Food*, 3(10), 862–870. <https://doi.org/10.1038/s43016-022-00613-9>

Feng, S., & Hao, Z. (2020). Quantifying likelihoods of extreme occurrences causing maize yield reduction at the global scale. *Science of the Total Environment*, 704, 135250. <https://doi.org/10.1016/j.scitotenv.2019.135250>

Feng, S., Hao, Z., Zhang, X., & Hao, F. (2019). Probabilistic evaluation of the impact of compound dry-hot events on global maize yields. *Science of the Total Environment*, 689, 1228–1234. <https://doi.org/10.1016/j.scitotenv.2019.06.373>

García-Herrera, R., Díaz, J., Trigo, R. M., Luterbacher, J., & Fischer, E. M. (2010). A review of the European summer heat wave of 2003. *Critical Reviews in Environmental Science and Technology*, 40(4), 267–306. <https://doi.org/10.1080/10643380802238137>

Glotter, M., & Elliott, J. (2016). Simulating US agriculture in a modern Dust Bowl drought. *Nature Plants*, 3(1), 16193. <https://doi.org/10.1038/nplants.2016.193>

Granier, A., Bréda, N., Biron, P., & Villette, S. (1999). A lumped water balance model to evaluate duration and intensity of drought constraints in forest stands. *Ecological Modelling*, 116(2), 269–283. [https://doi.org/10.1016/S0304-3800\(98\)00205-1](https://doi.org/10.1016/S0304-3800(98)00205-1)

Groemping, U. (2006). Relative importance for linear regression in R: The Package relaimpo. *Journal of Statistical Software*, 17(1), 1–27. <https://doi.org/10.18637/jss.v017.i01>

Groemping, U., & Matthias, L. (2018). Package “relaimpo”: Relative importance of regressors in linear models (R package version). Retrieved from <https://cran.r-project.org/web/packages/relaimpo/relaimpo.pdf>

Hamed, R., Van Loon, A. F., Aerts, J., & Coumou, D. (2021). Impacts of compound hot-dry extremes on US soybean yields. *Earth System Dynamics*, 12(4), 1371–1391. <https://doi.org/10.5194/esd-12-1371-2021>

Hamza, M., & Anderson, W. (2002). Improving soil physical fertility and crop yield on a clay soil in Western Australia. *Australian Journal of Agricultural Research*, 53(5), 615–620. <https://doi.org/10.1071/ar01099>

Han, J., Wang, J., Zhao, Y., Wang, Q., Zhang, B., Li, H., & Zhai, J. (2018). Spatio-temporal variation of potential evapotranspiration and climatic drivers in the Jing-Jin-Ji region, North China. *Agricultural and Forest Meteorology*, 256–257, 75–83. <https://doi.org/10.1016/j.agrformet.2018.03.002>

Hao, Z., Hao, F., Xia, Y., Feng, S., Sun, C., Zhang, X., et al. (2022). Compound droughts and hot extremes: Characteristics, drivers, changes, and impacts. *Earth-Science Reviews*, 235, 104241. <https://doi.org/10.1016/j.earscirev.2022.104241>

Haqiqi, I., Grogan, D. S., Hertel, T. W., & Schlenker, W. (2021). Quantifying the impacts of compound extremes on agriculture. *Hydrology and Earth System Sciences*, 25(2), 551–564. <https://doi.org/10.5194/hess-25-551-2021>

Harrison, M. T., Cullen, B. R., & Rawnsley, R. P. (2016). Modelling the sensitivity of agricultural systems to climate change and extreme climatic events. *Agricultural Systems*, 148, 135–148. <https://doi.org/10.1016/j.agsy.2016.07.006>

He, Y., Huang, W., Pu, Z., Li, M., Cheng, M., Liu, Y., et al. (2022). Temporal transcriptomes unravel the effects of heat stress on seed germination during wheat grain filling. *Journal of Agronomy and Crop Science*, 208(5), 709–720. <https://doi.org/10.1111/jac.12586>

Holzworth, D. P., Huth, N. I., deVoil, P. G., Zurcher, E. J., Herrmann, N. I., McLean, G., et al. (2014). APSIM—evolution towards a new generation of agricultural systems simulation. *Environmental Modelling & Software*, 62, 327–350. <https://doi.org/10.1016/j.envsoft.2014.07.009>

Hu, T., Van Dijk, A. I. J. M., Renzullo, L. J., Xu, Z., He, J., Tian, S., et al. (2020). On agricultural drought monitoring in Australia using Himawari-8 geostationary thermal infrared observations. *International Journal of Applied Earth Observation and Geoinformation*, 91, 102153. <https://doi.org/10.1016/j.jag.2020.102153>

Hussain, A., Memon, J. A., & Hanif, S. (2020). Weather shocks, coping strategies and farmers' income: A case of rural areas of district Multan, Punjab. *Weather and Climate Extremes*, 30, 100288. <https://doi.org/10.1016/j.wace.2020.100288>

Izumi, T., & Ramankutty, N. J. E. R. L. (2016). Changes in yield variability of major crops for 1981–2010 explained. *Climate Change*, 11(3), 034003. <https://doi.org/10.1088/1748-9326/11/3/034003>

Júnior, R. D. S. N., Martre, P., Finger, R., Van Der Velde, M., Ben-Ari, T., Ewert, F., et al. (2021). Extreme lows of wheat production in Brazil. *Environmental Research Letters*, 16(10), 104025. <https://doi.org/10.1088/1748-9326/ac26f3>

Kaye, J. P., & Quemada, M. (2017). Using cover crops to mitigate and adapt to climate change. A review. *Agronomy for sustainable development*, 37, 1–17. <https://doi.org/10.1007/s13593-016-0410-x>

Keating, B. A., Carberry, P. S., Hammer, G. L., Probert, M. E., Robertson, M. J., Holzworth, D., et al. (2003). An overview of APSIM, a model designed for farming systems simulation. *European Journal of Agronomy*, 18(3), 267–288. [https://doi.org/10.1016/S1161-0301\(02\)00108-9](https://doi.org/10.1016/S1161-0301(02)00108-9)

Keating, B. A., & Thorburn, P. J. (2018). Modelling crops and cropping systems—Evolving purpose, practice and prospects. *European Journal of Agronomy*, 100, 163–176. <https://doi.org/10.1016/j.eja.2018.04.007>

Khasawneh, M. A., & Al-Oqaily, D. M. (2023). Development of analytical models to predict the dynamic shear rheometer outcome—phase angle. *International Journal of Pavement Research and Technology*, 16(2), 425–443. <https://doi.org/10.1007/s42947-021-00141-y>

Kirkegaard, J. A., & Lilley, J. M. (2007). Root penetration rate a benchmark to identify soil and plant limitations to rooting depth in wheat %J Australian Journal of Experimental Agriculture. *Australian Journal of Experimental Agriculture*, 47(5), 590–602. <https://doi.org/10.1071/EA06071>

Kumar Tewari, A., & Charan Tripathy, B. (1998). Temperature-stress-induced impairment of chlorophyll biosynthetic reactions in cucumber and wheat. *Plant Physiology*, 117(3), 851–858. <https://doi.org/10.1104/pp.117.3.851>

Lalic, B., Eitzinger, J., Mihailovic, D., Thaler, S., & Jancic, M. J. T. J. O. a. S. (2013). Climate change impacts on winter wheat yield change—which climatic parameters are crucial in Pannonian lowland? *Journal of Agricultural Science*, 151(6), 757–774. <https://doi.org/10.1017/S0021859612000640>

Lesk, C., & Anderson, W. (2021). Decadal variability modulates trends in concurrent heat and drought over global croplands. *Environmental Research Letters*, 16(5), 055024. <https://doi.org/10.1088/1748-9326/abeb35>

Lesk, C., Anderson, W., Rigden, A., Coast, O., Jägermeyr, J., Mcdermid, S., et al. (2022). Compound heat and moisture extreme impacts on global crop yields under climate change. *Nature Reviews Earth & Environment*, 3(12), 872–889. <https://doi.org/10.1038/s43017-022-00368-8>

Lesk, C., Coffel, E., Winter, J., Ray, D., Zscheischler, J., Seneviratne, S. I., & Horton, R. (2021). Stronger temperature–moisture couplings exacerbate the impact of climate warming on global crop yields. *Nature Food*, 2(9), 683–691. <https://doi.org/10.1038/s43016-021-00341-6>

Lewis, F., Butler, A., & Gilbert, L. (2011). A unified approach to model selection using the likelihood ratio test. *Methods in Ecology and Evolution*, 2, 155–162. <https://doi.org/10.1111/j.2041-210X.2010.00063.x>

Li, E., Zhao, J., Pullens, J. W. M., & Yang, X. (2022a). The compound effects of drought and high temperature stresses will be the main constraints on maize yield in Northeast China. *Science of the Total Environment*, 812, 152461. <https://doi.org/10.1016/j.scitotenv.2021.152461>

Li, S. (2024a). Paper\_EF\_data (version 1) [Dataset]. *Zenodo*. <https://doi.org/10.5281/zenodo.12492673>

Li, S. (2024b). Paper\_EF\_software (version 1) [Software]. *Zenodo*. <https://doi.org/10.5281/zenodo.12493289>

Li, S., Wang, B., Feng, P., Liu, D. L., Li, L., Shi, L., & Yu, Q. (2022b). Assessing climate vulnerability of historical wheat yield in south-eastern Australia's wheat belt. *Agricultural Systems*, 196, 103340. <https://doi.org/10.1016/j.agysy.2021.103340>

Li, S., Wang, B., Liu, D. L., Chao, C., Feng, P., Mingxia, H., et al. (2024). Can agronomic options alleviate the risk of compound drought-heat events during wheat flowering period in southeastern Australia? *European Journal of Agronomy*, 153, 127030. <https://doi.org/10.1016/j.eja.2023.127030>

Liu, D. L., Timbal, B., Mo, J., & Fairweather, H., & Management. (2011). A GIS-based climate change adaptation strategy tool. *International Journal of Climate Change Strategies and Management*, 3(2), 140–155. <https://doi.org/10.1108/1756869111128986>

Liu, D. L., Wang, B., Evans, J., Ji, F., Waters, C., Macadam, I., et al. (2019). Propagation of climate model biases to biophysical modelling can complicate assessments of climate change impact in agricultural systems. *International Journal of Climatology*, 39(1), 424–444. <https://doi.org/10.1002/joc.5820>

Lobell, D. B., Hammer, G. L., Chenu, K., Zheng, B., Mclean, G., & Chapman, S. C. (2015). The shifting influence of drought and heat stress for crops in northeast Australia. *Global Change Biology*, 21(11), 4115–4127. <https://doi.org/10.1111/gcb.13022>

Luan, X., Bommarco, R., Scaini, A., & Vico, G. (2021). Combined heat and drought suppress rainfed maize and soybean yields and modify irrigation benefits in the USA. *Environmental Research Letters*, 16(6), 064023. <https://doi.org/10.1088/1748-9326/abfc76>

Madagdar, S., Aghakouchak, A., Farahmand, A., & Davis, S. J. (2017). Probabilistic estimates of drought impacts on agricultural production. *Geophysical Research Letters*, 44(15), 7799–7807. <https://doi.org/10.1002/2017GL073606>

Mangani, R., Tesfamariam, E. H., Engelbrecht, C. J., Bellocchi, G., Hassen, A., & Mangani, T. (2019). Potential impacts of extreme weather events in main maize (*Zea mays* L.) producing areas of South Africa under rainfed conditions. *Regional Environmental Change*, 19(5), 1441–1452. <https://doi.org/10.1007/s10113-019-01486-8>

Manning, C., Widmann, M., Bevacqua, E., Van Loon, A. F., Maraun, D., & Vrac, M. J. E. R. L. (2019). Increased probability of compound long-duration dry and hot events in Europe during summer (1950–2013). *Environmental Research Letters*, 14(9), 094006. <https://doi.org/10.1088/1748-9326/ab23bf>

Marcellos, H., & Single, W. (1975). Temperatures in wheat during radiation frost. *Australian Journal of Experimental Agriculture*, 15(77), 818–822. <https://doi.org/10.1071/EA9750818>

Misaghian, N., Assareh, M., & Sadeghi, M. (2018). An upscaling approach using adaptive multi-resolution upgridding and automated relative permeability adjustment. *Computational Geosciences*, 22(1), 261–282. <https://doi.org/10.1007/s10596-017-9688-2>

Murtaugh, P. A. (2014). In defense of P values. *Ecology*, 95(3), 611–617. <https://doi.org/10.1890/13-0590.1>

Myhre, G., Alterskjær, K., Stjern, C. W., Hodnebrog, Ø., Marelle, L., Samset, B. H., et al. (2019). Frequency of extreme precipitation increases extensively with event rareness under global warming. *Scientific Reports*, 9(1), 16063. <https://doi.org/10.1038/s41598-019-52277-4>

Nix, H. A., & Fitzpatrick, E. A. (1969). An index of crop water stress related to wheat and grain sorghum yields. *Agricultural Meteorology*, 6(5), 321–337. [https://doi.org/10.1016/0002-1571\(69\)90024-7](https://doi.org/10.1016/0002-1571(69)90024-7)

Padarian, J., Minasny, B., Mcbratney, A. B., & Dalglish, N. (2014). Predicting and mapping the soil available water capacity of Australian wheatbelts. *Geoderma Regional*, 2–3, 110–118. <https://doi.org/10.1016/j.geodrs.2014.09.005>

Potopová, V., Lhotka, O., Možný, M., & Musiolková, M. (2021). Vulnerability of hop-yields due to compound drought and heat events over European key-hop regions. *International Journal of Climatology*, 41(S1), E2136–E2158. <https://doi.org/10.1002/joc.6836>

Ribeiro, A. F. S., Russo, A., Gouveia, C. M., Páscoa, P., & Zscheischler, J. J. B. (2020). Risk of crop failure due to compound dry and hot extremes estimated with nested copulas. *Biogeosciences*, 17(19), 4815–4830. <https://doi.org/10.5194/bg-17-4815-2020>

Roberts, M. J., Braun, N. O., Sinclair, T. R., Lobell, D. B., & Schlenker, W. (2017). Comparing and combining process-based crop models and statistical models with some implications for climate change. *Environmental Research Letters*, 12(9), 095010. <https://doi.org/10.1088/1748-9326/aa7f33>

Rötter, R. P., Tao, F., Höhn, J. G., & Palosuo, T. (2015). Use of crop simulation modelling to aid ideotype design of future cereal cultivars. *Journal of Experimental Botany*, 66(12), 3463–3476. <https://doi.org/10.1093/jxb/erv098>

Sarhadi, A., Ausin, M. C., Wiper, M. P., Touma, D., & Diffenbaugh, N. S. (2018). Multidimensional risk in a nonstationary climate: Joint probability of increasingly severe warm and dry conditions. *Science Advances*, 4(11), eaau3487. <https://doi.org/10.1126/sciadv.aau3487>

Schauberger, B., Gornott, C., & Wechsung, F. (2017). Global evaluation of a semiempirical model for yield anomalies and application to within-season yield forecasting. *Global Change Biology*, 23(11), 4750–4764. <https://doi.org/10.1111/gcb.13738>

Semenov, M. A., & Strattonovich, P. J. C. R. (2015). Adapting wheat ideotypes for climate change: Accounting for uncertainties in CMIP5 climate projections. *Climate Research*, 65, 123–139. <https://doi.org/10.3354/cr01297>

SILO. (2023). Long Paddock, 2023, Home LongPaddock | Queensland Government.

Simanjuntak, C., Gaiser, T., Ahrends, H. E., Ceglar, A., Singh, M., Ewert, F., & Srivastava, A. K. (2023). Impact of climate extreme events and their causality on maize yield in South Africa. *Scientific Reports*, 13(1), 12462. <https://doi.org/10.1038/s41598-023-38921-0>

Single, W. (1985). Frost injury and the physiology of the wheat plant. *Journal of the Australian Institute of Agricultural Science*.

Stagge, J. H., Tallaksen, L. M., Gudmundsson, L., Van Loon, A. F., & Stahl, K. (2015). Candidate distributions for climatological drought indices (SPI and SPEI). *International Journal of Climatology*, 35(13), 4027–4040. <https://doi.org/10.1002/joc.4267>

Steinskog, D. J., Tjøstheim, D. B., & Kvamstø, N. G. (2007). A cautionary note on the use of the Kolmogorov–Smirnov test for normality. *Monthly Weather Review*, 135(3), 1151–1157. <https://doi.org/10.1175/MWR3326.1>

Stone, P., & Nicolas, M. (1994). Wheat cultivars vary widely in their responses of grain yield and quality to short periods of post-anthesis heat stress. *Functional Plant Biology*, 21(6), 887–900. <https://doi.org/10.1071/PP9940887> %.

Telfer, P., Edwards, J., Bennett, D., Ganesalingam, D., Able, J., & Kuchel, H. (2018). A field and controlled environment evaluation of wheat (*Triticum aestivum*) adaptation to heat stress. *Field Crops Research*, 229, 55–65. <https://doi.org/10.1016/j.fcr.2018.09.013>

van der Velde, M., Tubiello, F. N., Vrieling, A., & Bouraoui, F. (2012). Impacts of extreme weather on wheat and maize in France: Evaluating regional crop simulations against observed data. *Climatic Change*, 113(3–4), 751–765. <https://doi.org/10.1007/s10584-011-0368-2>

Vogel, E., Donat, M. G., Alexander, L. V., Meinshausen, M., Ray, D. K., Karoly, D., et al. (2019). The effects of climate extremes on global agricultural yields. *Environmental Research Letters*, 14(5), 054010. <https://doi.org/10.1088/1748-9326/ab154b>

Wang, A., Tao, H., Ding, G., Zhang, B., Huang, J., & Wu, Q. (2023). Global cropland exposure to extreme compound drought heatwave events under future climate change. *Weather and Climate Extremes*, 40, 100559. <https://doi.org/10.1016/j.wace.2023.100559>

Wang, B., Feng, P., Waters, C., Cleverly, J., Liu, D. L., & Yu, Q. (2020). Quantifying the impacts of pre-occurred ENSO signals on wheat yield variation using machine learning in Australia. *Agricultural and Forest Meteorology*, 291, 108043. <https://doi.org/10.1016/j.agrformet.2020.108043>

Wang, B., Li Liu, D., Waters, C., & Yu, Q. (2018). Quantifying sources of uncertainty in projected wheat yield changes under climate change in eastern Australia. *Climatic Change*, 151(2), 259–273. <https://doi.org/10.1007/s10584-018-2306-z>

Wang, B., Liu, D. L., Asseng, S., Macadam, I., & Yu, Q. (2017). Modelling wheat yield change under CO<sub>2</sub> increase, heat and water stress in relation to plant available water capacity in eastern Australia. *European Journal of Agronomy*, 90, 152–161. <https://doi.org/10.1016/j.eja.2017.08.005>

Wang, B., Liu, D. L., O'leary, G. J., Asseng, S., Macadam, I., Lines-Kelly, R., et al. (2018). Australian wheat production expected to decrease by the late 21st century. *Global Change Biology*, 24(6), 2403–2415. <https://doi.org/10.1111/gcb.14034>

Wardlaw, I. F., Blumenthal, C., Larroque, O., & Wrigley, C. W. (2002). Contrasting effects of chronic heat stress and heat shock on kernel weight and flour quality in wheat. *Functional Plant Biology*, 29(1), 25–34. <https://doi.org/10.1071/PP00147>

Watson, J., Zheng, B., Chapman, S., & Chenu, K. (2017). Projected impact of future climate on water-stress patterns across the Australian wheatbelt. *Journal of Experimental Botany*, 68(21–22), 5907–5921. <https://doi.org/10.1093/jxb/erx368>

Wegren, S. K. (2011). Food Security and Russia's 2010 Drought. *Eurasian Geography and Economics*, 52(1), 140–156. <https://doi.org/10.2747/1539-7216.52.1.140>

Wheeler, T. R., Batts, G. R., Ellis, R. H., Hadley, P., & Morison, J. I. L. (1996). Growth and yield of winter wheat (*Triticum aestivum*) crops in response to CO<sub>2</sub> and temperature. *The Journal of Agricultural Science*, 127(1), 37–48. <https://doi.org/10.1017/S002185960007732>

Xie, Z., Zhao, Y., Jiang, R., Zhang, M., Hammer, G., Chapman, S., et al. (2024). Seasonal dynamics of fallow and cropping lands in the broadacre cropping region of Australia. *Remote Sensing of Environment*, 305, 114070. <https://doi.org/10.1016/j.rse.2024.114070>

Yuan, X., Wang, L., & Wood, E. F. (2018). Anthropogenic intensification of southern African flash droughts as exemplified by the 2015/16 season. *Bulletin of the American Meteorological Society*, 99(1), S86–S90. <https://doi.org/10.1175/bams-d-17-0077.1>

Zampieri, M., Ceglar, A., Dentener, F., & Toreti, A. J. E. R. L. (2017). Wheat yield loss attributable to heat waves, drought and water excess at the global, national and subnational scales. *Environmental Research Letters*, 12(6), 064008. <https://doi.org/10.1088/1748-9326/aa723b>

Zheng, B., Chenu, K., Fernanda Drecer, M., & Chapman, S. C. (2012). Breeding for the future: What are the potential impacts of future frost and heat events on sowing and flowering time requirements for Australian bread wheat (*Triticum aestivum*) varieties? *Global Change Biology*, 18(9), 2899–2914. <https://doi.org/10.1111/j.1365-2486.2012.02724.x>

Zscheischler, J., Martius, O., Westra, S., Bevacqua, E., Raymond, C., Horton, R. M., et al. (2020). A typology of compound weather and climate events. *Nature Reviews Earth & Environment*, 1(7), 333–347. <https://doi.org/10.1038/s43017-020-0060-z>

Zwiers, F. W., Alexander, L. V., Hegerl, G. C., Knutson, T. R., Kossin, J. P., Naveau, P., et al. (2013). Climate extremes: Challenges in estimating and understanding recent changes in the frequency and intensity of extreme climate and weather events. In *Climate Science for Serving Society: Research, Modeling and Prediction Priorities* (pp. 339–389). Springer Netherlands.